Microbial Biosynthesis of Rare Cannabinoids

Chunsheng Yan,[1] Ikechukwu C. Okorafor,[1,3]* Colin W. Johnson,[2] K. N. Houk,[2] Neil K. Garg,[2] Yi Tang [1,2]*

[1] Department of Chemical and Biomolecular Engineering, [2] Department of Chemistry and Biochemistry, [3] California NanoSystems Institute, University of California, Los Angeles, CA 90095, USA.

ABSTRACT

Δ^9–tetrahydrocannabinol (Δ^9–THC) and cannabidiol (CBD) are the most abundant natural cannabinoids isolated from the different cultivars of the *Cannabis* plant. Other natural Δ^9–THC analogs, especially those with different alkyl chain substitutions, display different and potent bioactivity. However, these rare cannabinoids are typically isolated at minuscule amounts and are difficult to synthesize. Targeted microbial biosynthesis can therefore be an attractive route to access such molecules. Here, we report the development of a *Saccharomyces cerevisiae* host to biosynthesize two rare cannabinoids from simple sugars. The yeast host is engineered to accumulate excess geranyl pyrophosphate (GPP), to overexpress a fungal pathway to 2,4-dihydroxy-6-alkyl-benzoic acids, as well as the downstream UbiA-prenyltransferase and THCA synthase. Two rare cannabinoid acids, the C1-substituted Δ^9–tetrahydrocannabiorcolic acid (Δ^9–THCCA, ~16 mg/L) and the C7-substituted Δ^9 –tetrahydrocannabiphorolic acid (Δ^9 –THCPA, ~5 mg/L) were obtained from this host; the latter was thermally decarboxylated to give Δ^9-tetrahydrocannabiphorol (Δ^9 –THCP). Given the diversity of fungal biosynthetic gene clusters (BGCs) that can produce resorcylic acids, this microbial platform offers potential to produce other rare and new-to-nature cannabinoids.

INTRODUCTION

Cannabinoids are a large class of bioactive natural products that interact with the cannabinoid receptors of the human endocannabinoid system.[1] The most abundant and well-known natural cannabinoids are Δ^9–tetrahydrocannabinol (Δ^9–THC) and cannabidiol (CBD), isolated from different cultivars of the *Cannabis* plant. Cannabinoid-based medicines (CBMs) have shown promise as pharmacological agents, acting as antidepressants, analgesics, anticonvulsants, and antiemetics.[2] Two cannabinoid-based medicines, cesamet (nabilone), an antiemetic for cancer chemotherapy,[3] and dronabinol, an antiemetic that also treats appetite loss, are currently on the market.[4] Rare cannabinoids with different alkyl chain substitutions instead of the five-carbon (C5) chain in Δ^9–THC and CBD have been isolated from plant sources,[5-11] some of which display stronger affinity toward human CB_1 receptors than Δ^9–THC (Figure 1). For example, Δ^9–tetrahydrocannabutol (Δ^9–THCB) with a butyl (C4) chain and Δ^9-tetrahydrocannabiphorol (Δ^9–THCP) with a heptyl (C7) chain display K_i values of 15 nM[7] and 1.2 nM,[9] respectively, against human CB1 receptor *in* vitro, which correspond to ~5-fold and 30-fold stronger inhibition compared to that of Δ^9–THC (K_i = 40 nM) [9]. While these natural, rare cannabinoids are attractive lead molecules for CBMs, the low abundance of these molecules poses significant challenges to scalable isolation.[12] From dried and decarboxylated raw plant materials, ~ 30 mg/g of the most abundant cannabinoid Δ^9–THC can be isolated.[13] In contrast, the compositions of other Δ^9–THC analogs are all below 1 mg/g (Figure 1).[7,9,10,14] Synthetic methods for accessing the cannabinoid molecules have been developed, but remain difficult to implement at scale due to the complexities involved in the multistep reactions.[15] As a result, synthetic biology approaches utilizing microbial hosts are attractive options for obtaining rare and new-to-nature cannabinoid molecules.

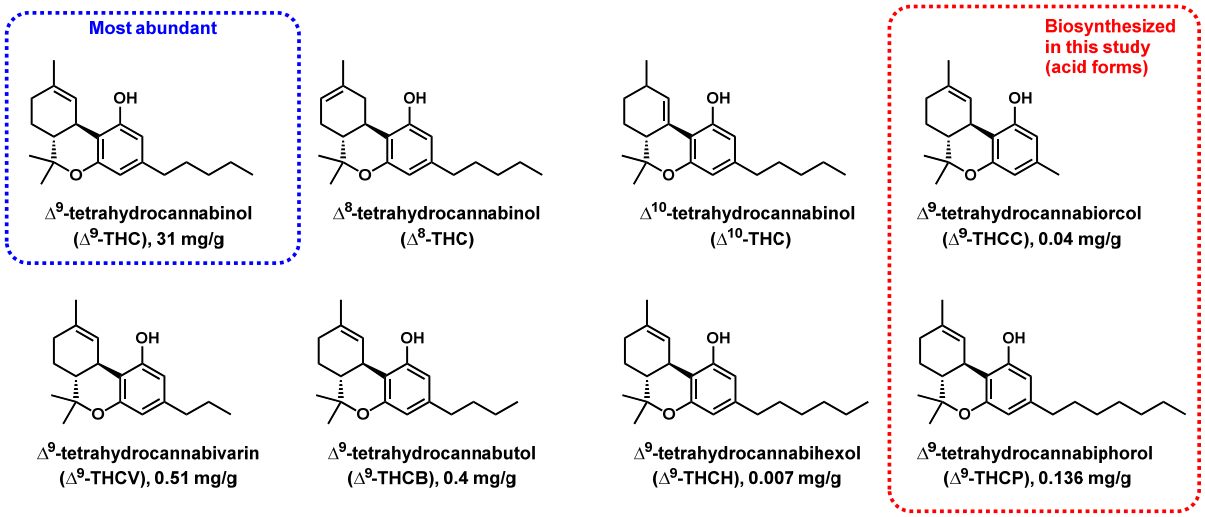

Figure 1. Δ^9–THC and other natural Δ^9–THC analogs isolated from natural *Cannabis* plant. The reported titers per g of plant biomass are listed. The acid forms of two rare analogs, Δ^9–THCCA and Δ^9–THCPA, are biosynthesized from yeast in this work.

Various strategies toward engineering microbes to produce cannabinoids have been reported since the identification of *Cannabis sativa L.* plant olivetolic acid synthase (OLS) and

olivetolic acid cyclase (OAC),[16] which collectively synthesize olivetolic acid (OA), the C5 substituted resorcylic acid intermediate (Figure 2). Gonzalez and coworkers achieved 80 mg/L production of OA upon overexpression of OLS and OAC in *E. coli*.[17] In a cell-free synthetic biology approach, Bowie and coworkers engineered a *Streptomyces* prenyltransferase, NphB, to geranylate OA regioselectively to produce cannabigerolic acid (CBGA).[18] Keasling and coworkers identified a *Cannabis sativa* prenyltransferase, CsPT4, that natively performs *C*-geranylation of OA to CBGA. Further co-expression with tetrahydrocannabinolic acid cyclase (THCAS)[19] enabled reconstitution of the complete cannabinoid pathway in *S. cerevisiae* that produced 8 mg/L of Δ^9-tetrahydrocannabinolic acid (Δ^9–THCA), with 1.2 mg/L Δ^9-tetrahydrocannabivarinic acid (Δ^9–THCVA) produced as a side product (Figure S1).[20] This yeast system was further improved to increase precursor supply and CsPT4 function to produce CBGA at 510 mg/L.[21] All these engineering efforts are based on the plant pathway and aimed to improve the production of the two major precursors, hexanoyl-CoA and geranyl pyrophosphate (GPP).

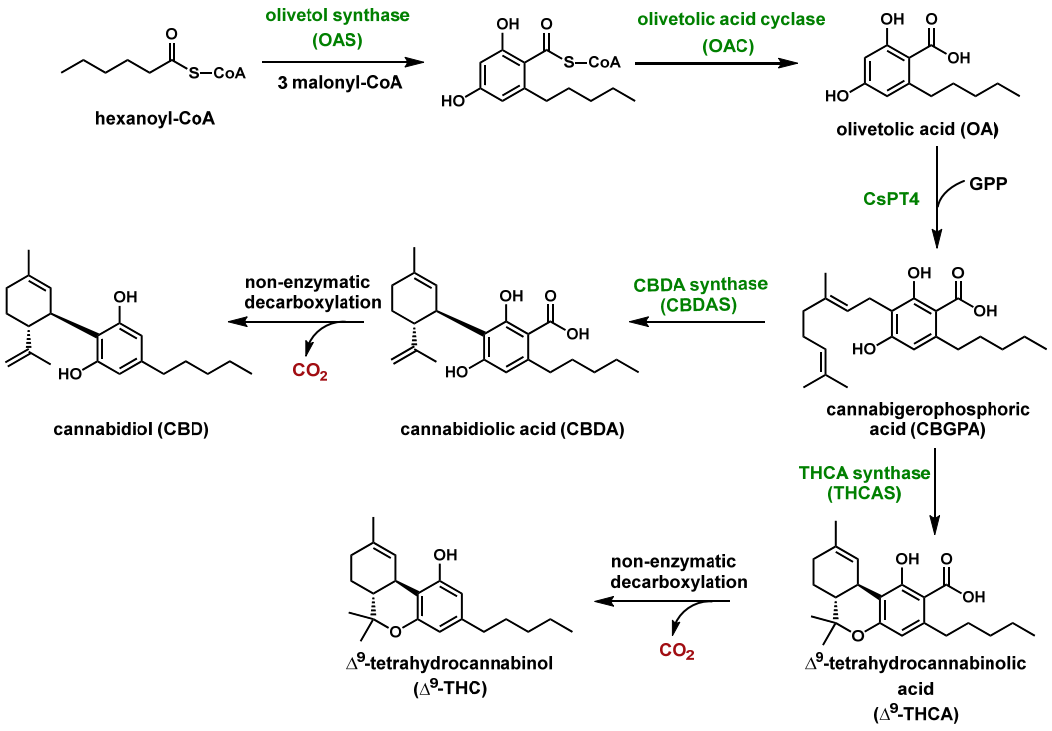

Figure 2. The plant biosynthetic pathway to CBD and Δ^9–THC. The pathway has been introduced into microbes for partial and complete pathway expression.

Our laboratory previously reported a fungal biosynthetic pathway that can synthesize OA and other alkyl-substituted 2,4-dihydroxybenzoic acids. The three-enzyme pathway, derived from *Metarhizium anisopliae*, consists of a highly reducing polyketide synthase (HRPKS, Ma_OvaA) that generates the alkyl chain starter unit, a nonreducing polyketide synthase (NRPKS, Ma_OvaB) that elongates and cyclizes the starter unit into the 2,4-dihydroxy-6-alkyl benzoyl-thioester, and a thioesterase (Ma_OvaC) that releases the product (Figure 3A).[22] When heterologously expressed in the *Aspergillus nidulans* A1145 ΔSTΔEM host,[23] the pathway produced the C7

sphaerophorolcarboxylic acid (SA) with a titer of 1.4 g/L, along with OA at 80 mg/L, and unsaturated analogs of SA and OA, which are **1** (~140 mg/L) and **2** (0.4 mg/L), respectively (Figure 3B).[22] This fungal biosynthetic pathway therefore provides direct access to SA at high titer and can be a starting point to access the rare but highly potent C7 Δ^9–THCP (Figure 1).[9] In this report, we demonstrate the reconstitution of this pathway in an engineered yeast host, which enabled the *in vivo* production of Δ^9-tetrahydrocannabiphorolic acid (Δ^9–THCPA) that can be subsequently decarboxylated to Δ^9–THCP**,** along with the unexpected production of C1-substituted Δ^9–tetrahydrocannabiorcolic acid (Δ^9–THCCA).

RESULTS AND DISCUSSION

Attempted Pathway Engineering in A. nidulans

Upon expressing the biosynthetic gene cluster containing the Ma_OvaABC genes in *A. nidulans*, multiple OA analogs were produced (Figure 3B). Extension of this pathway with coexpression of prenyltransferase and the cyclase THCAS should therefore lead to CBGA and THCA analogs. To investigate if prenylation reaction can be reconstituted, a thermal stabilized version of the bacterial prenyltransferase NphB, engineered for efficient prenylation of OA to CBGA,[18] was expressed in *A. nidulans* with Ma_OvaABC (Figure 3B). Upon metabolite analysis, NphB did not prenylate OA or other alkyl-substituted 2,4-dihydroxybenzoic acids. Previous reports suggested the soluble ABBA-type prenyltransferase NphB is highly active *in vitro*,[18] but activity is significantly reduced when expressed in *Komagataella phaffii*.[24] We hypothesized that the soluble NphB may be localized in the cytoplasm of *A. nidulans* and therefore has limited access to the key substrate, geranyl pyrophosphate, produced by the mevalonate pathway, which involves ER-localized enzymes and other enzymes localized in different cellular regions.[25] To investigate the subcellular localization of NphB in *A. nidulans*, we performed intracellular localization analysis by fusing NphB to a C-terminal green fluorescent protein (GFP). A flexible amino acid linker (GGSGG) sequence was inserted between NphB and GFP.[26] Microscopic images of the tagged NphB enzyme in *A. nidulans* showed that NphB was not localized in any punctuate organelles but rather was distributed throughout the fungal body indicating that the enzyme is located in the cytoplasm, which potentially limits access to GPP substrate and hence lack of prenylation activity in *A. nidulans* (Figure S2).

CsPT4 is a *Cannabis* plant enzyme that belongs to the UbiA-family of membrane bound prenyltransferases. This enzyme was shown to catalyze geranylation of OA in yeast to afford CBGA.[20] To assess its activity in *A. nidulans*, we coexpressed a truncated CsPT4 without the plastid targeting sequence (tCsPT4) with Ma_OvaABC in *A. nidulans*.[20] However, no prenylated products were observed (Figure 3B). *A. nidulans* was previously used for monoterpene and diterpene production, indicating there is sufficient GPP in the host.[27] Furthermore, using a monoterpene pathway as a test, we verified that GPP supply is available in the fungal host (data not shown). *A. nidulans* has not been commonly used for the heterologous expression of plant-

derived enzymes, which may be due to different intracellular environment or localization compared to plant hosts. These factors may affect the stability of heterologous enzymes such as tCsPT4. Collectively, we concluded that further attempts to extend the cannabinoid pathway in *A. nidulans* are not warranted and decided to move the pathway into the yeast *S. cerevisiae.*

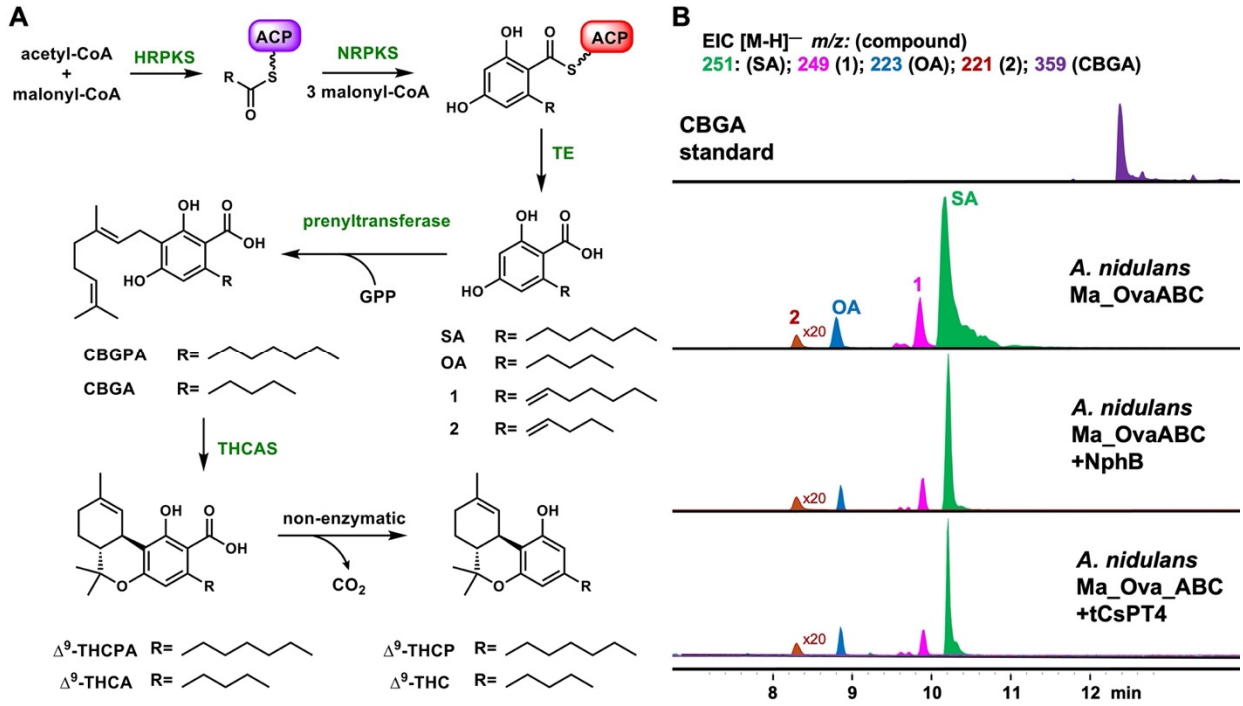

Figure 3. Proposed pathway to access rare cannabinoids such as Δ^9–THCPA with the C7 side chain. (**A**) Proposed extension of the biosynthetic pathway involving Ma_OvaABC to produce Δ^9–THC and analogs; (**B**) Metabolic analysis from the heterologous expression of Ma_OvaABC and tCsPT4, NphB in *A. nidulans* shows the prenyltransferases do not function in the fungal host.

Pathway Engineering in yeast

The Ma_OvaABC pathway was first expressed in the *S. cerevisiae* strain JHY686, a strain derived from the integration of the *A. nidulans* phosphopantetheinyl (pPant) transferase into the chromosome of the JHY651 strain (Table S3).[28] Each enzyme was expressed from an autoinducible ADH promoter on a 2μ plasmid.[29] The resulting yeast strain, after 4 days of culturing in YPD media, was extracted and analyzed for metabolite production (Figure 4). Multiple 2,4-dihydroxybenzoic acid compounds, including OA, SA, **1,** and a compound with molecular weight identical to orsellinic acid (OsA) were detected. The titer of the most abundant compound, SA, was determined to be ~ 500 mg/L in this unoptimized strain. Although the titer is lower than that in *A. nidulans* (1.4 g/L), the robust biosynthesis of SA in yeast is an encouraging first step in downstream pathway construction.

Co-expression of NphB with Ma_OvaABC in JHY686 again did not produce any prenylated products (Figure 3). However, coexpression of tCsPT4 with Ma_OvaABC led to the production of CBGA (as compared to a standard) and two new compounds with MWT of 388 (~5

mg/L) and 456 (~8 mg/L). To elucidate the structures of the two compounds, large-scale yeast culturing (5 x 800 mL) was performed followed by purification. Full NMR characterization revealed that the compound with MWT of 388 was indeed geranylated SA product cannabigerophorolic acid (CBGPA) (Table S4, Figures S5-10), while the compound with MWT of 456 was the farnesylated SA (**3**) derived from transfer of farnesyl group from farnesyl diphosphate (FPP) to SA (Figure 3, Table S7, Figures S23-28). Successful prenylation of OA and SA in the yeast host, albeit incomplete, led us to coexpress THCAS with Ma_OvaABC and tCsPT4 as the next step.

THCAS has been demonstrated to cyclize prenylated OA analogs with varying alkyl chain lengths, including CBGA (C5) and CBGVA (C3).[20] Upon introducing plasmid expressing THCAS targeted to the vacuole of JHY686,[24] tCsPT4, and Ma_OvaABC in JHY686, selected ion monitoring of *m/z* $[M-H]^-$ 385 led to the appearance of trace amounts of a compound that could be Δ^9–THCPA (Figure 4). The low titer (estimated to be < 100 μg/L) hindered isolation of the compound for complete NMR analysis.

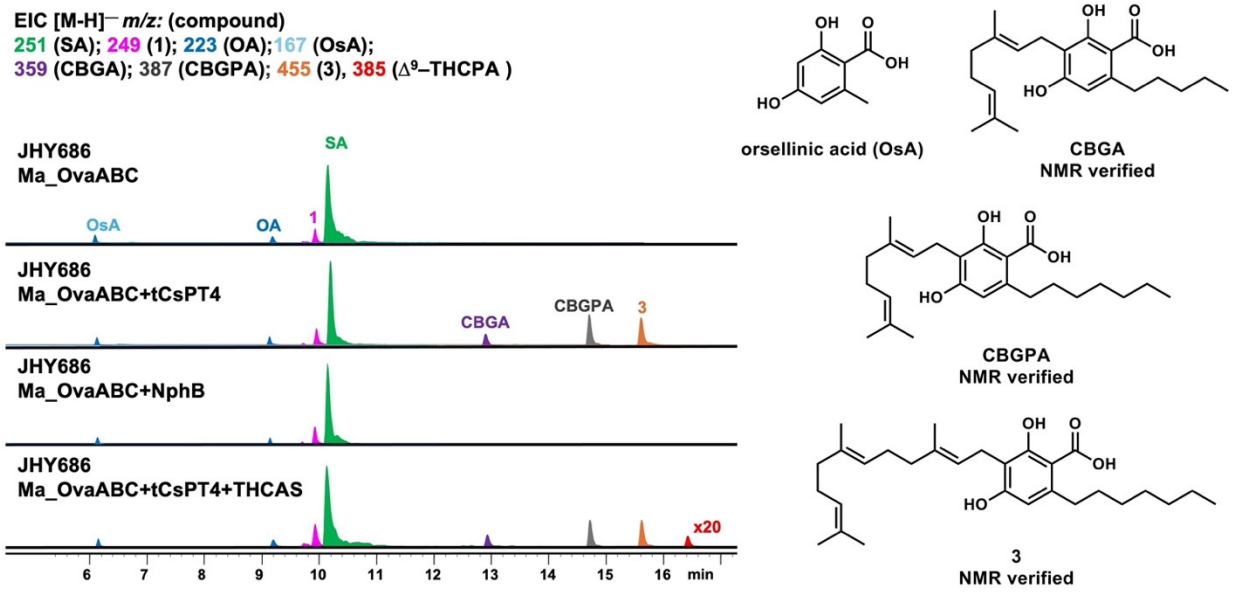

Figure 4. Heterologous expression Ma_OvaABC, tCsPT4 and THCAS in *S. cerevisiae* JHY686 strain. Expression of Ma_OvaABC in JHY686 resulted in production of SA. Co-expression of tCsPT4 with Ma_OvaABC led to the biosynthesis of CBGPA along with the farnesyl pyrophosphate (FPP)-derived shunt product **3**. The presence of orsellinic acid (OsA) was proposed based on the molecular weight and UV absorbance. The structures of the isolatable compounds are verified by NMR. In contrast, co-expression of NphB with Ma_OvaABC did not lead to prenylated products. Co-expression of tCsPT4 and THCAS with Ma_OvaABC led to trace amounts of a compound with MWT of 386, same as Δ^9–THCPA.

Improving Δ^9–THCPA production from yeast and non-enzymatic decarboxylation to Δ^9–THCP

Examining the distribution of products from the yeast strain that expresses all enzymes, it is clear that geranylation of SA to CBGPA, and the oxidative cyclization of CBGPA to Δ^9–THCPA,

are both highly inefficient in yeast. To address the first issue, we hypothesized that the free GPP pool in yeast is not sufficient to support high titer CBGPA formation. The low intracellular GPP concentration in yeast is well documented, and numerous approaches have been developed.[30] Based on these approaches, we first integrated additional copies of genes encoding key enzymes from the mevalonate pathway into the yeast chromosome, including those encoding truncated 3-hydroxy-3-methylglutaryl-coenzymeA reductase (tHMG1) and isopentenyl-diphosphate delta isomerase 1 (IDI1). Furthermore, the mutated FPP synthases from *S. cerevisiae* (ERG20*K197G) and the *Gallus gallus* (mFPS*N144W) were integrated to increase GPP accumulation, and to arrive at the strain yIO002 (for detailed strain genotype, see Table S3).[28] Coexpression of tCsPT4 with Ma_OvaABC in yIO02 resulted in increased titer of CBGPA (~30 mg/L) (Figure 5). However, a substantial increase in the titer of the FPP-derived shunt product **3** (~150 mg/L) was also observed (Figure 4 and Figure S4), suggesting this shunt pathway diverts the flux of the desired pathway. Subsequently, coexpression of tCsPT4 and THCAS with Ma_OvaABC in yIO02 resulted in an improved titer (~1 mg/L) of the compound with MWT of 386 (Figure 5). This increase in titer enabled production and isolation from larger scale yeast cultures. Complete NMR analysis confirmed that the compound is indeed the expected Δ^9–THCPA (Table S5, Figures S11-16).

The low conversion of CBGPA to Δ^9–THCPA was attributed to the elevated temperature of the yeast cultures, which is typically performed at 28°C. Previous expression of THCAS using *Pichia pastoris* as a host showed the enzyme expressed optimally when expression was induced at 15°C. [31] Therefore, to further increase Δ^9–THCPA production, culturing conditions were tuned by varying temperature to achieve a balance of yeast metabolic activity, tCsPT4 activity and THCAS activity. The best condition achieved was first culturing the yeast at 15°C for three days to allow proper expression and folding of THCAS, followed by increasing the temperature to 28°C for four days to elevate the cellular metabolic activity. A five-fold increase in the titer of Δ^9–THCPA (~5 mg/L) was achieved under these conditions, with **3** remaining as the major shunt product (Figures 5 and S4). Keeping the temperature at 15°C for the entire duration of the culture did not lead to formation of any related products.

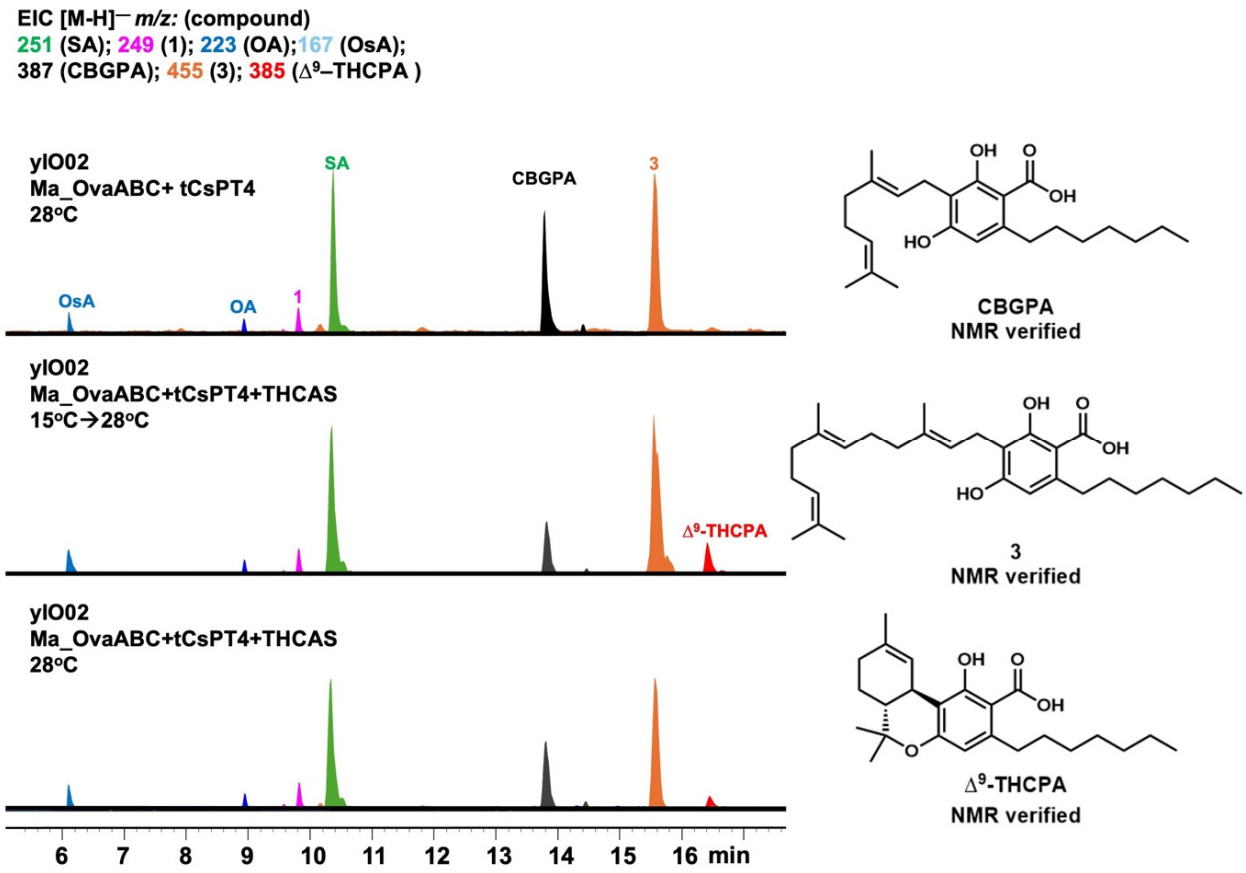

Figure 5. Metabolic analysis of heterologous expression of Ma_OvaABC, tCsPT4, and THCAS in yIO02 strain that has elevated intracellular GPP levels. The optimal condition is when the cells were initially cultured at 15°C for 3 days, followed by an incubation at 28°C for an additional 4 days. The titer of Δ^9–THCPA reached ~ 5 mg/L under this condition. **3**, which is the farnesylated analog of CBGPA remains a major shunt product under all conditions.

Non-enzymatic decarboxylation of Δ^9–THCP

The conversion of Δ^9–THCPA to the potent cannabinoid Δ^9–THCP involves thermal decarboxylation that is non-enzymatic. By drying the purified Δ^9–THCPA sample and heating at 130°C for 1 hour, > 90% conversion to Δ^9 –THCP was achieved.[32] The final product was structurally verified by NMR characterization (Table S6, Figures S17-22). Δ^9–THCP was first isolated from *Cannabis FM2 strain* in 2019 and was demonstrated to have 30 times higher affinity to the human CB_1 receptor and 5-10 times higher affinity to the human CB_2 receptor, when compared to those of Δ^9–THC.[9] Our microbial platform, with minimal optimization, is able to produce the immediate precursor to this molecule at ~ 5 mg/L, compared to the ~ 0.13 mg/g of Δ^9–THCP isolated from the producing plant.

Structural modeling to understand prenyl donor promiscuity of CsPT4

The accumulation of shunt product **3** with the farnesyl group indicates CsPT4 is promiscuous towards the prenyl donors, which is consistent with previous reports.[33] Given FPP is more abundant in yeast and **3** is a dead-end product, such promiscuity depletes the pool of SA that can be geranylated for the biosynthesis of CBGPA and ultimately Δ^9–THCPA. It should be noted, however, C3-farnesyl-CBGA exhibits anti-neuroinflammatory and antibacterial activities,[34] suggesting that **3** could also exhibit potential bioactivities. In order to understand the molecular basis for substrate recognition, we performed structural analysis of tCsPT4 using Alphafold 3 accompanied with docking with GPP substrate and comparison to reported UbiA-prenyltransferase structures.[35] The archaeal membrane-bound UbiA prenyltransferase (PDB: 4OD4) was crystalized with *p*-hydroxybenzoate (PHB) and GPP.[36] The crystal structure revealed a large and hydrophobic active site where GPP was cocrystalized, providing structural basis to the observed prenyl donor promiscuity (Figure 6A). Similarly, the predicted structural prediction of tCsPT4 revealed a similar, large hydrophobic cavity. The binding pocket of CsPT4 comprises of two distinct parts: one region is rich in aspartic acid which can bind phosphate and Mg^{2+}; and a small opening which is the prenyl-binding chamber. The Alphafold predicted structure and docking results indicate that tCsPT4 could indeed accommodate longer prenyl substrates such as FPP (Figure 6B and Figure S4). Comprehensive mutation screening of the prenyl binding pocket can be deployed to identify tCsPT4 mutants that can exclude FPP in favor of GPP. Recently, a promiscuous prenyltransferase AscC was engineered to display improved prenyl donor selectivity through site-directed mutagenesis.[34]

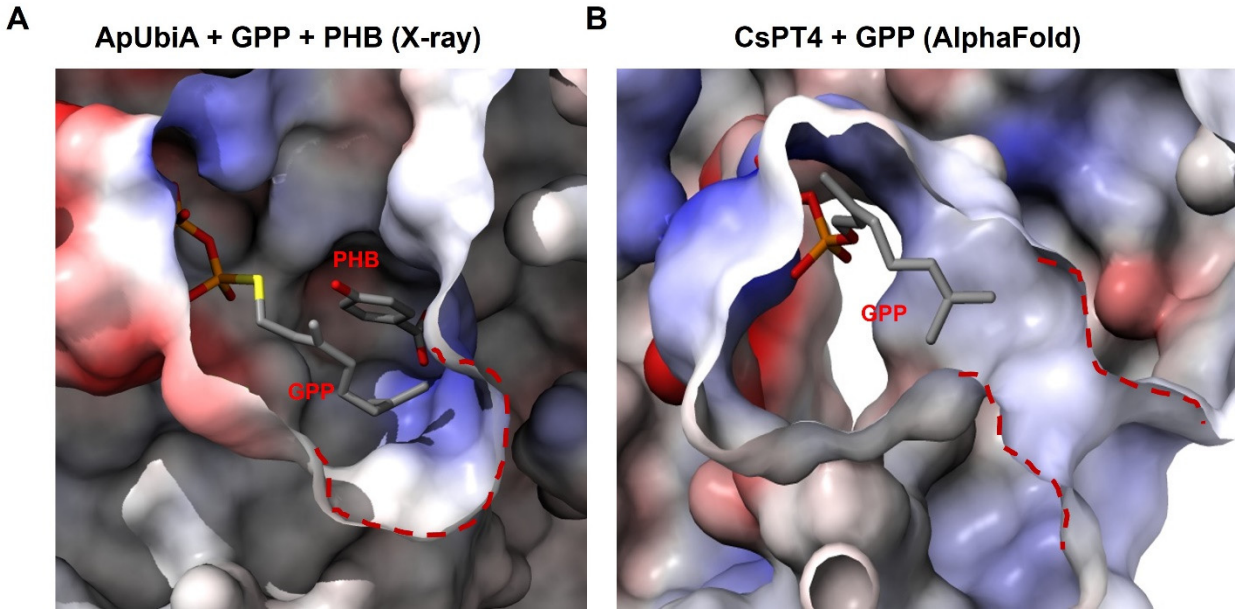

Figure 6. Electrostatic representation of the binding pockets of (**A**) ApUbiA (PDB: 4OD5) and (**B**) CsPT4. The CsPT4 structure was predicted by Alphafold 3, and docking was performed by replica-exchange Monte Carlo simulation.[37]

Genome mining for a fungal prenyltransferase with OsA as substrate

Expression of Ma_OvaABC in yIO02 and JHY686 resulted in the production of a compound with molecular weight and UV absorbance consistent with that of orsellinic acid (OsA) (Figure 4). The biosynthesis of OsA by Ma_OvaABC in yeast was unexpected, as this compound was not observed in *A. nidulans* (Figure 3B). OsA is a 2,4-dihydroxybenzoic acid with a C1 substitution, which biosynthetically can be synthesized from the NRPKS after priming by acetyl-CoA. We therefore attribute the formation of OsA to the direct priming of Ma_OvaB in yeast and bypassing the octanoyl starter unit provided by the HRPKS Ma_OvaA. Nevertheless, the formation of OsA can be exploited for the biosynthesis of the corresponding C1 analog of Δ^9–THCA, Δ^9–tetrahydrocannabiorcolic acid (Δ^9–THCCA). The decarboxylated product of Δ^9–THCCA, Δ^9–THCC, is a very rare cannabinoid isolated from *Cannabis sativa L.* Unlike most other cannabinoids that bind to CB_1 and CB_2 receptors, Δ^9 –THCC has negligible affinity to CB_1 and CB_2 but functions as an activator of the TRPA1 calcium channel which plays an integral role in pain perception.[14,38]

In the yeast transformant that produced CBGPA (Figure 4), the geranylated cannabigerorcinic acid (CBGCA) and Δ^9–THCCA were not detected, suggesting tCsPT4 could not prenylate OsA. Hence, a OsA-specific prenyltransferase is required. Based on the lack of function with bacterial prenyltransferases in fungi, we reasoned a fungal prenyltransferase is more likely to be functionally expressed in yeast. With this in mind, we sought to identify previously isolated 2,4-dihydroxybenzoic acid fungal metabolites with *C*-prenylation at the C-3 position. A particular group of related prenylated orsellinaldehyde derivatives was particularly attractive with respect to enzyme mining (Figure 7A). A number of such derivatives are reported from the various plant pathogens, but in particular, the colletorins and chlorinated colletochlorins isolated from *Colletotrichum* species of the Destructivum complex (*C. nicotinae, C. destructivum, C. higginsianum*) were notable in that in multiple accounts these organisms produced major isolated products that are *C*-geranylated.[39,40,41,42] Based on these reports, the prenyltransferase involved in the biosynthesis of the colletorins and colletochlorins can be a potential candidate for predominantly geranylating the C-3 position amongst a diverse prenyl-donor pool.

To identify the desired colletorin BGC harboring our target prenyltransferase, we first set out to define a minimum BGC based on the structural constituents of the colletorins and structurally related products. The proposed pathway includes formation of the orsellinic acid core by an NRPKS, which is modified by an ensemble of a prenyltransferase, a halogenase, and a reductase. Searching available *Colletotrichum* genomes within the Destructivum complex (namely *C. destructivum and C. higginsianum*) resulted in only one such BGC that meets these criteria, which we named as the *col* BGC (Figure 7A). The *col* BGC is comprised of genes that encode an NRPKS (*colC*), an NRPS-like enzyme with the domain architecture adenylation (A)-thiolation (T)-reductase (R) (*colB*), a halogenase (*colD*), and an UbiA-prenyltransferase (*colA*) (Figure 7A). The proposed sequence of reactions catalyzed by these enzymes are shown in Figure 7B.

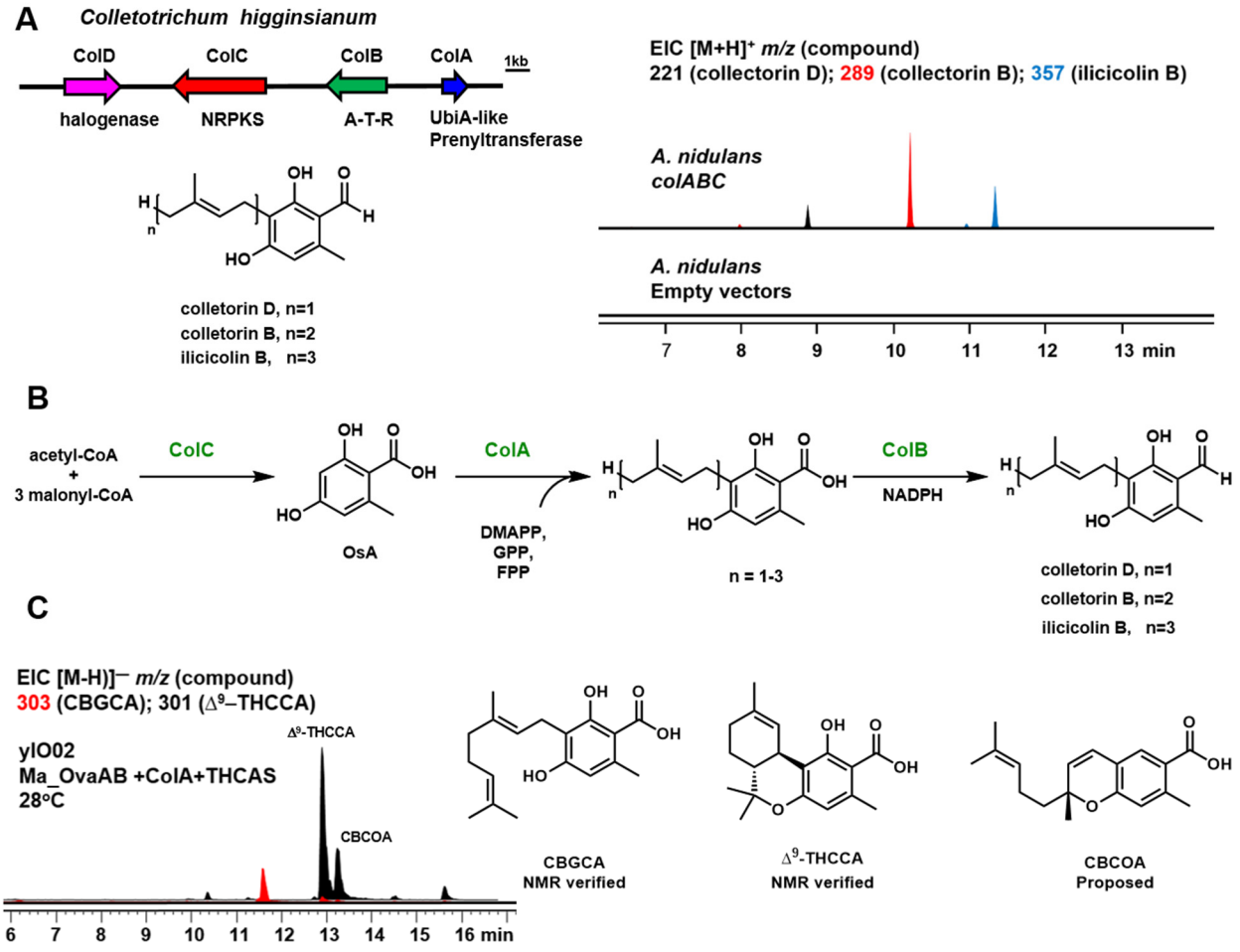

Figure 7. Discovery of the fungal UbiA prenyltransferase, ColA, and application for biosynthesis of THCCA. (**A**) The fungal biosynthetic gene cluster containing ColA, and metabolic analysis of heterologous expression of *col* gene cluster in *A. nidulans*. (ATR domains: adenylation-thiolation-reductase). The control trace is the metabolic analysis of the *A. nidulans* expressing empty vectors. From the metabolic analysis of *A. nidulans* expressing genes *colABC*, the transformation produced compounds with equivalent MWT to colletorin D, colletorin B and ilicicolin B. (**B**) The proposed biosynthetic pathway of the colletorin products; (**C**) Metabolic analysis of heterologous expression of ColA with Ma_OvaABC and THCAS in yIO02. Two new metabolites with MWT 304 and 302 are produced, which were NMR verified to be CBGCA and Δ^9–THCCA, respectively. A third metabolite with MWT of 302 is proposed to be CBGOA.

To test our hypothesis, we heterologously expressed the *col* cluster in *A. nidulans*. The transformant expressing the ColB, ColC and the prenyltransferase ColA produced compounds with the same MWTs of colletorin D, colletorin B and ilicicolin B (Figure 7A), at a ratio of 1:5:2. In terms of the relative retention time and UV absorbance, we proposed that the three new compounds are the colletorin compounds with different prenyl groups. These heterologous expression results indicated that WT ColA could not only effectively prenylate OsA but also yielded more of the desired geranylated product compared to the farnesylated compound. To determine if ColA can be integrated into the yeast strain to produce Δ^9–THCCA, ColA was coexpressed with Ma_OvaABC and THCAS in yIO02 (Figures 7C). The yeast transformant was then cultured with

temperature shift condition previously detailed. Two new compounds with MWT of 304 and 302, which match that of CBGCA and Δ^9–THCCA, respectively, were found in the extracts. Large-scale yeast culture was performed followed by purification of the compounds. Complete NMR analysis confirmed the two compounds are indeed CBGCA (Table S8, Figures S29-34) and Δ^9–THCCA (~16 mg/L) (Table S9, Figure S4 and Figures S35-40). An additional metabolite with MWT 302 was also identified in addition to the major product Δ^9–THCCA (Figure 7C). This minor product was proposed to be cannabichromeorcinic acid (CBCOA) based on the production of CBCA in additional to Δ^9–THC from CBGA catalyzed by THCAS.[43]

CONCLUSION

In summary, we have engineered *S. cerevisiae* to achieve *de novo* biosynthesis of two rare cannabinoids, Δ^9–THCPA (~5 mg/L) and Δ^9–THCCA (~16 mg/L). The engineered pathways include fungal enzymes for biosynthesis of the 2,4-dihydroxy-6-alkylbenzoic acid core; either a plant or a fungal prenyltransferase for regioselective prenylation; and the plant THCAS for oxidative cyclization to the cannabinoid. The titers were improved with increased GPP production and optimized temperature conditions. There remains significant room for further optimization, especially with regard to the prenyl donor promiscuity of tCsPT4. Our work demonstrates this yeast platform can be flexible in combining different enzymes to access rare cannabinoids. With the diversity of fungal BGCs capable of producing 2,4-dihydroxylbenzoic acid or resorcylic acid natural products, additional rare cannabinoids can be produced, especially those containing different alkyl chains.

METHODS

Plasmids and strains

E. coli TOP10 was used for cloning, following standard recombinant DNA techniques. DNA restriction enzymes were used as recommended from the manufacturer (New England Biolabs, NEB). Q5 High Fidelity DNA polymerase (NEB) is used for all PCR reactions. The plasmids were sequenced by Laragen and Primordium Lab. Gene integrations and deletions were performed through CRISPR-Cas9 unless otherwise noted using the protocol described from Horwitz et al.[44] Guide RNA sequences were designed with the CRISPRy Cas9 target finder.[45] Plasmids with gRNA sequences contained *hygR* or *kanMX* antibiotic resistance markers. The primers used in this study are listed in Table S1. Plasmids used for cloning are listed in Table S2. Strain genotypes are listed in Table S3. Knockouts were performed using antibiotic markers. To remove GES from previous engineered strain S12 (Table S3), a hygromycin marker flanked with 30-60 bp homology to CrGES was transformed into the S12 strain to remvoe CrGES. The knockout was confirmed by plating on selection plate containing hygromycin and by sequencing the knockout region. A zeocin marker flanked with 30-60 bp homology to ObGES was transformed to

knockout ObGES. The double knockout strain was confirmed by plating on plates containing hygromycin and zeocin and by sequencing of both knockout regions.

Three plasmid vectors, pYTU, pYTP, and pYTR containing auxotrophic markers for uracil (*pyrG*), pyridoxine (*pyroA*), and riboflavin (*riboB*) respectively were used to construct plasmids for *A. nidulans* heterologous expression. *gpdA* promoters from *Penicillium oxalicum* (constitutive *POgpdA*), *A. niger* (constitutive *gpdA*, *glaA* induced by starch) and *Penicillium expansum* (constitutive *PEgpdA*) were amplified by PCR. pYTP and pYTR were digested with *PacI*/*NotI*. pYTU was digested with *PacI*/*NotI* (keep *glaA* on vector) or *PShAI*/*NotI* (abolish glaA from vector). The amplified gene fragments and the corresponding vectors were co-transformed into *S. cerevisiae* JHY651 for homologous recombination. The yeast plasmids were extracted using Zymoprep™ Yeast Plasmid Miniprep I (Zymo Inc. USA), and then electrically transformed into *E. coli* TOP10 to isolate single plasmids. The plasmids were extracted from *E. coli* using the Zyppy™ Plasmid Miniprep Kit (Zymo Research).

Yeast culturing for metabolite production

Single colonies of each strain were inoculated in 1 mL YPD. For plasmid bearing strains, single colony transformants were inoculated in 1 mL synthetic defined (SD) 2% glucose media with the appropriate dropouts. Starter cultures were shaken at 28°C and 250 rpm for 16–24 hr. Culture tubes containing 2 mL of fresh YPD with 100 µL of starter culture. For cannabinoid acid production, the culture was incubated at 15°C, 220 rpm for 3 days and then changed to at 28°C, 220 rpm for 4 days. For large-scale extraction, a single transformant colony was picked into 1 mL selection media incubated at 28°C, 220 rpm overnight. Then 1 mL seed culture was transferred into 40mL selection media incubated at 28°C, 220 rpm overnight. Then 40 mL seed culture was transferred into 800 mL YPD for isolation of the products. For THCPA production, the culture was incubated at 15°C, 220 rpm for 3 days and then changed to 28°C, 220 rpm for 4 days.

Culture extraction and quantification, and structural determination

For small scale yeast culture extraction, 300 µL culture sample was extracted with 300 µL organic phase consisting of 25% acetone and 75% ethyl acetate with 0.1% FA for three times. The samples were vortexed for 1 min then centrifuged for 10 min. All the extracts were dried, and the residues were dissolved in MeOH for analysis. LC-MS analyses were performed on a Shimadzu 2020 EV LC-MS with a reverse phase column (Phenomenex Kinetex 1.7 µm C18 100 Å, LC Column 100 × 2.1 mm) using positive-and negative-mode electrospray ionization with a linear gradient of 5–95% CH_3CN-H_2O with 0.1% formic acid (v/v) in 15 min followed by 95% CH_3CN for 3 min with a flow rate of 0.3 ml/min and a 6545 Q-TOF high resolution mass spectrometer (UCLA Molecular Instrumentation Center) using the solvent program (1% CH_3CN-H_2O 2 min, then 1-95% CH_3CN-H_2O (both with 0.1% formic acid, v/v) in 9 min followed by 95% CH_3CN-H_2O for 6 min at a flow rate of 0.8 mL/min).

To isolate sufficient amount of compound for NMR analysis, large-scale yeast culture was performed and the cells were separated by centrifugation. The cell pellet was extracted by acetone and the supernatant was extracted by EtOAc. The extracts were dried, combined and then redissolved in 15 mL methanol. The insoluble impurities were discarded. 10 g of celite was added to the mixture and methanol was evaporated. The dried crude was purified with the CombiFlash system (Teledyne) using reverse phase gradient elution with water (A) and acetonitrile (B) with 0.1% FA. The fractions containing desired product were dried and then redissolved in methanol. Semi-preparative HPLC was performed on an S7 UltiMateTM 3000 Semi-Preparative HPLC (ThermoFisher) using a COMOSIL 5C18-AR-II (5 μm, 4.6 × 250 mm) or COSMOSIL 5C18-MS-II column (5 μm, 250 ×10 mm). Flow rate for HPLC was set at 3 mL/min. NMR spectra were obtained with a Bruker AV500 spectrometer with a 5 mm dual cryoprobe at the UCLA Molecular Instrumentation Center (^{1}H NMR 500 MHz, ^{13}C NMR 125 MHz).

Quantification of the compounds was performed by first making a standard curve on the HPLC. Known concentrations of isolated compound were analyzed on the HPLC (ThermoFisher), and a standard curve was constructed correlating the area under the UV peak corresponding to the compound to the concentration of the compound. Cultured samples were then extracted and analyzed on the HPLC, where the area under the peak was used to calculate the concentration of the sample.

ACKNOWLEDGMENT

We are grateful to the California Department of Cannabis Control (Grant Agreement Number: 93414) for financial support of this research. Chemical characterization studies were supported by shared instrumentation grants from the NSF (CHE-1048804) and the NIH NCRR (S10RR025631). CY is supported by NIGMS predoctoral fellowship, 5T32GM136614.

REFERENCES

1. Pertwee, R. G. Cannabinoid Pharmacology: The First 66 Years. *Br. J. Pharmacol.* **2006**, *147* (S1).
2. Devinsky, O.; Cilio, M. R.; Cross, H.; Fernandez-Ruiz, J.; French, J.; Hill, C.; Katz, R.; Di Marzo, V.; Jutras-Aswad, D.; Notcutt, W. G.; Martinez-Orgado, J.; Robson, P. J.; Rohrback, B. G.; Thiele, E.; Whalley, B.; Friedman, D. Cannabidiol: Pharmacology and Potential Therapeutic Role in Epilepsy and Other Neuropsychiatric Disorders. *Epilepsia* **2014**, *55* (6), 791–802.
3. Dalzell, A. M.; Bartlett, H.; Lilleyman, J. S. Nabilone: An Alternative Antiemetic for Cancer Chemotherapy. *Arch. Dis. Child.* **1986**, *61* (5), 502–505.
4. Patar, A. K.; Borah, S. M.; Barman, J.; Bora, A.; Baruah, T. J. Dronabinol as an Answer to Flavivirus Infections: An in-Silico Investigation. *J. Biomol. Struct. Dyn.* **2023**, *41* (20), 11219–11230.
5. Hanus, Lumir; Zd, Krejci. Isolation of two new cannabinoid acids from Cannabis sativa L. of Czechoslovak origin. *Acta Universitatis Palackianae Olomucensis Facultatis Medicae*. **1975**, 161-166.
6. Srebnik, M.; Lander, N.; Breuer, A.; Mechoulam, R. Base-Catalysed Double-Bond Isomerizations of Cannabinoids: Structural and Stereochemical Aspects. *J. Chem. Soc., Perkin Trans. 1* **1984**, 2881.
7. Linciano, P.; Citti, C.; Luongo, L.; Belardo, C.; Maione, S.; Vandelli, M. A.; Forni, F.; Gigli, G.; Laganà, A.; Montone, C. M.; Cannazza, G. Isolation of a High-Affinity Cannabinoid for the Human CB1 Receptor from a Medicinal *Cannabis Sativa* Variety: Δ^9-Tetrahydrocannabutol, the Butyl Homologue of Δ^9-Tetrahydrocannabinol. *J. Nat. Prod.* **2020**, *83* (1), 88–98.
8. Gill, E. W.; Paton, W. D. M.; Pertwee, R. G. Preliminary Experiments on the Chemistry and Pharmacology of Cannabis. *Nature* **1970**, *228* (5267), 134–136.
9. Citti, C.; Linciano, P.; Russo, F.; Luongo, L.; Iannotta, M.; Maione, S.; Laganà, A.; Capriotti, A. L.; Forni, F.; Vandelli, M. A.; Gigli, G.; Cannazza, G. A Novel Phytocannabinoid Isolated from Cannabis Sativa L. with an in Vivo Cannabimimetic Activity Higher than Δ9-Tetrahydrocannabinol: Δ9-Tetrahydrocannabiphorol. *Sci. Rep.* **2019**, *9* (1).
10. Linciano, P.; Citti, C.; Russo, F.; Tolomeo, F.; Laganà, A.; Capriotti, A. L.; Luongo, L.; Iannotta, M.; Belardo, C.; Maione, S.; Forni, F.; Vandelli, M. A.; Gigli, G.; Cannazza, G. Identification of a New Cannabidiol N-Hexyl Homolog in a Medicinal Cannabis Variety with an Antinociceptive Activity in Mice: Cannabidihexol. *Sci. Rep.* **2020**, *10* (1).
11. Adams, R.; Loewe, S.; Smith, C. M.; McPhee, W. D. Tetrahydrocannabinol Homologs and Analogs with Marihuana Activity. XIII[1]. *J. Am. Chem. Soc.* **1942**, *64* (3), 694–697.
12. ElSohly, M. A.; Gul, W. Constituents of Cannabis Sativa. In *Handbook of Cannabis*; Oxford University Press, 2014; pp 3–22.

13. Backman, I. *Marijuana: Rising THC concentrations in cannabis can pose health risks*. Yale.edu (accessed 2025-03-06).
14. Ross, S. A.; ElSohly, M. A.; Sultana, G. N. N.; Mehmedic, Z.; Hossain, C. F.; Chandra, S. Flavonoid Glycosides and Cannabinoids from the Pollen of Cannabis Sativa L. *Phytochem. Anal.* **2005**, *16* (1), 45–48.
15. Bloemendal, V. R. L. J.; van Hest, J. C. M.; Rutjes, F. P. J. T. Synthetic Pathways to Tetrahydrocannabinol (THC): An Overview. *Org. Biomol. Chem.* **2020**, *18* (17), 3203–3215.
16. Gülck, T.; Møller, B. L. Phytocannabinoids: Origins and Biosynthesis. *Trends Plant Sci.* **2020**, *25* (10), 985–1004.
17. Tan, Z.; Clomburg, J. M.; Gonzalez, R. Synthetic Pathway for the Production of Olivetolic Acid in *Escherichia Coli*. *ACS Synth. Biol.* **2018**, *7* (8), 1886–1896.
18. Valliere, M. A.; Korman, T. P.; Arbing, M. A.; Bowie, J. U. A Bio-Inspired Cell-Free System for Cannabinoid Production from Inexpensive Inputs. *Nat. Chem. Biol.* **2020**, *16* (12), 1427–1433.
19. Sirikantaramas, S.; Morimoto, S.; Shoyama, Y.; Ishikawa, Y.; Wada, Y.; Shoyama, Y.; Taura, F. The Gene Controlling Marijuana Psychoactivity. *J. Biol. Chem.* **2004**, *279* (38), 39767–39774.
20. Luo, X.; Reiter, M. A.; d'Espaux, L.; Wong, J.; Denby, C. M.; Lechner, A.; Zhang, Y.; Grzybowski, A. T.; Harth, S.; Lin, W.; Lee, H.; Yu, C.; Shin, J.; Deng, K.; Benites, V. T.; Wang, G.; Baidoo, E. E. K.; Chen, Y.; Dev, I.; Petzold, C. J.; Keasling, J. D. Complete Biosynthesis of Cannabinoids and Their Unnatural Analogues in Yeast. *Nature* **2019**, *567* (7746), 123–126.
21. Zhang, Y.; Guo, J.; Gao, P.; Yan, W.; Shen, J.; Luo, X.; Keasling, J. D. Development of an Efficient Yeast Platform for Cannabigerolic Acid Biosynthesis. *Metab. Eng.* **2023**, *80*, 232–240.
22. Okorafor, I. C.; Chen, M.; Tang, Y. High-Titer Production of Olivetolic Acid and Analogs in Engineered Fungal Host Using a Nonplant Biosynthetic Pathway. *ACS Synth. Biol.* **2021**, *10* (9), 2159–2166.
23. Yee, D. A.; Tang, Y. Investigating Fungal Biosynthetic Pathways Using Heterologous Gene Expression: Aspergillus Nidulans as a Heterologous Host. In *Methods in Molecular Biology*; Springer US: New York, NY, 2022; pp 41–52.
24. Zirpel, B.; Degenhardt, F.; Martin, C.; Kayser, O.; Stehle, F. Engineering Yeasts as Platform Organisms for Cannabinoid Biosynthesis. *J. Biotechnol.* **2017**, *259*, 204–212.
25. Orban, A. M.; Rühl, M. Identification of Volatile Producing Enzymes in Higher Fungi: Combining Analytical and Bioinformatic Methods. *Methods Enzymol.* **2022**, *664*, 221–242.
26. Chen, X.; Zaro, J. L.; Shen, W.-C. Fusion Protein Linkers: Property, Design and Functionality. *Adv. Drug Deliv. Rev.* **2013**, *65* (10), 1357–1369.

27. Bromann, K.; Toivari, M.; Viljanen, K.; Ruohonen, L.; Nakari-Setälä, T. Engineering Aspergillus Nidulans for Heterologous Ent-Kaurene and Gamma-Terpinene Production. *Appl. Microbiol. Biotechnol.* **2016**, *100* (14), 6345–6359.
28. Yee, D. A.; DeNicola, A. B.; Billingsley, J. M.; Creso, J. G.; Subrahmanyam, V.; Tang, Y. Engineered Mitochondrial Production of Monoterpenes in Saccharomyces Cerevisiae. *Metab. Eng.* **2019**, *55*, 76–84.
29. Harvey, C. J. B.; Tang, M.; Schlecht, U.; Horecka, J.; Fischer, C. R.; Lin, H.-C.; Li, J.; Naughton, B.; Cherry, J.; Miranda, M.; Li, Y. F.; Chu, A. M.; Hennessy, J. R.; Vandova, G. A.; Inglis, D.; Aiyar, R. S.; Steinmetz, L. M.; Davis, R. W.; Medema, M. H.; Sattely, E.; Khosla, C.; St Onge, R. P.; Tang, Y.; Hillenmeyer, M. E. HEx: A Heterologous Expression Platform for the Discovery of Fungal Natural Products. *Sci. Adv.* **2018**, *4* (4), eaar5459.
30. Chen, R.; Yang, S.; Zhang, L.; Zhou, Y. J. Advanced Strategies for Production of Natural Products in Yeast. *iScience* **2020**, *23* (3), 100879.
31. Zirpel, B.; Stehle, F.; Kayser, O. Production of Δ9-Tetrahydrocannabinolic Acid from Cannabigerolic Acid by Whole Cells of Pichia (Komagataella) Pastoris Expressing Δ9-Tetrahydrocannabinolic Acid Synthase from Cannabis Sativa l. *Biotechnol. Lett.* **2015**, *37* (9), 1869–1875.
32. Wang, M.; Wang, Y.-H.; Avula, B.; Radwan, M. M.; Wanas, A. S.; van Antwerp, J.; Parcher, J. F.; ElSohly, M. A.; Khan, I. A. Decarboxylation Study of Acidic Cannabinoids: A Novel Approach Using Ultra-High-Performance Supercritical Fluid Chromatography/Photodiode Array-Mass Spectrometry. *Cannabis Cannabinoid Res.* **2016**, *1* (1), 262–271.
33. Tanaya, R.; Kodama, T.; Lee, Y.-E.; Yasuno, Y.; Shinada, T.; Takahashi, H.; Ito, T.; Morita, H.; Awale, S.; Taura, F. Catalytic Potential of *Cannabis* Prenyltransferase to Expand Cannabinoid Scaffold Diversity. *Org. Lett.* **2023**, *25* (48), 8601–8605.
34. Yan, Q.; Chen, Y.-G.; Yang, X.-W.; Wang, A.; He, X.-P.; Tang, X.; Hu, H.; Guo, K.; Xiao, Z.-H.; Liu, Y.; Li, S.-H. Engineering a Promiscuous Prenyltransferase for Selective Biosynthesis of an Undescribed Bioactive Cannabinoid Analog. *Commun. Biol.* **2025**, *8* (1).
35. Abramson, J.; Adler, J.; Dunger, J.; Evans, R.; Green, T.; Pritzel, A.; Ronneberger, O.; Willmore, L.; Ballard, A. J.; Bambrick, J.; Bodenstein, S. W.; Evans, D. A.; Hung, C.-C.; O'Neill, M.; Reiman, D.; Tunyasuvunakool, K.; Wu, Z.; Žemgulytė, A.; Arvaniti, E.; Beattie, C.; Bertolli, O.; Bridgland, A.; Cherepanov, A.; Congreve, M.; Cowen-Rivers, A. I.; Cowie, A.; Figurnov, M.; Fuchs, F. B.; Gladman, H.; Jain, R.; Khan, Y. A.; Low, C. M. R.; Perlin, K.; Potapenko, A.; Savy, P.; Singh, S.; Stecula, A.; Thillaisundaram, A.; Tong, C.; Yakneen, S.; Zhong, E. D.; Zielinski, M.; Žídek, A.; Bapst, V.; Kohli, P.; Jaderberg, M.; Hassabis, D.; Jumper, J. M. Accurate Structure Prediction of Biomolecular Interactions with AlphaFold 3. *Nature* **2024**, *630* (8016), 493–500.
36. Cheng, W.; Li, W. Structural Insights into Ubiquinone Biosynthesis in Membranes. *Science* **2014**, *343* (6173), 878–881.

37. Zhang, W.; Bell, E. W.; Yin, M.; Zhang, Y. EDock: Blind Protein–Ligand Docking by Replica-Exchange Monte Carlo Simulation. *J. Cheminform.* **2020**, *12* (1).
38. Andersson, D. A.; Gentry, C.; Alenmyr, L.; Killander, D.; Lewis, S. E.; Andersson, A.; Bucher, B.; Galzi, J.-L.; Sterner, O.; Bevan, S.; Högestätt, E. D.; Zygmunt, P. M. TRPA1 Mediates Spinal Antinociception Induced by Acetaminophen and the Cannabinoid Δ9-Tetrahydrocannabiorcol. *Nat. Commun.* **2011**, *2* (1).
39. Sasaki, H.; Hosokawa, T.; Nawata, Y.; Ando, K. Isolation and Structure of Ascochlorin and Its Analogs. *Agric. Biol. Chem.* **1974**, *38* (8), 1463–1466.
40. Kosuge, Y.; Suzuki, A.; Tamura, S. Structures of Colletochlorin C, Colletorin A and Colletorin C from*Colletotrichum Nicotianae*. *Agric. Biol. Chem.* **1974**, *38* (6), 1265–1267.
41. Ellestad, G. A.; Evans, R. H., Jr; Kunstmann, M. P. Some New Terpenoid Metabolites from an Unidentified Fusarium Species. *Tetrahedron* **1969**, *25* (6), 1323–1334.
42. Kosuge, Y.; Suzuki, A.; Tamura, S. Structure of Colletochlorin D from*Colletotrichum Nicotianae*. *Agric. Biol. Chem.* **1974**, *38* (8), 1553–1554.
43. Zirpel, B.; Kayser, O.; Stehle, F. Elucidation of Structure-Function Relationship of THCA and CBDA Synthase from Cannabis sativaL. *J. Biotechnol.* **2018**, *284*, 17–26.
44. Horwitz, A. A.; Walter, J. M.; Schubert, M. G.; Kung, S. H.; Hawkins, K.; Platt, D. M.; Hernday, A. D.; Mahatdejkul-Meadows, T.; Szeto, W.; Chandran, S. S.; Newman, J. D. Efficient Multiplexed Integration of Synergistic Alleles and Metabolic Pathways in Yeasts via CRISPR-Cas. *Cell Syst.* **2015**, *1* (1), 88–96.
45. Jakočiūnas, T.; Bonde, I.; Herrgård, M.; Harrison, S. J.; Kristensen, M.; Pedersen, L. E.; Jensen, M. K.; Keasling, J. D. Multiplex Metabolic Pathway Engineering Using CRISPR/Cas9 in Saccharomyces Cerevisiae. *Metab. Eng.* **2015**, *28*, 213–222.

GRAPHICAL ABSTRACT

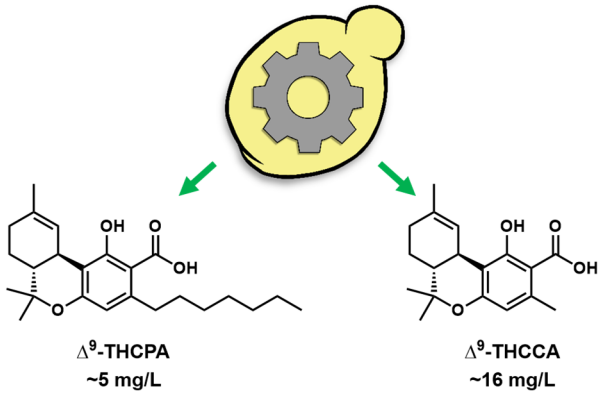

Supporting Information

Microbial Biosynthesis of Rare Cannabinoids

Chunsheng Yan,[1] Ikechukwu C. Okorafor,[1,3]* Colin W. Johnson,[2] K. N. Houk,[2] Neil K. Garg,[2] Yi Tang [1,2]*

[1] Department of Chemical and Biomolecular Engineering, [2] Department of Chemistry and Biochemistry, [3] California NanoSystems Institute, University of California, Los Angeles, CA 90095, USA.

Table of Contents

Experimental procedures

1. **Strains and culture conditions**

Aspergillus nidulans (*A. nidulans*) A1145 ΔSTΔEM was grown at 28 ºC on CD agar (1 L: 10 g glucose, 50 mL of 20X nitrate salts, 1 mL of trace elements, 20 g agar) or CDST agar (if use *glaA* promoter, 20 g starch, 20 g casamino acids (acidic digest), 50 mL 20X nitrate salts, 1 mL trace elements, 20 g agar) for heterologous expression of the gene cluster. The 20X nitrate salts are prepared as: 120 g of $NaNO_3$, 10.4 g of KCl, 10.4 g of $MgSO_4 \cdot 7H_2O$, 30.4 g of KH_2PO_4 dissolved in 1 L distilled water. The trace element solution was prepared as: 2.20 g of $ZnSO_4 \cdot 7H_2O$, 1.10 g of H_3BO_3, 0.50 g of $MnCl_2 \cdot 4H_2O$, 0.16 g of $FeSO_4 \cdot 7H_2O$, 0.16 g of $CoCl_2 \cdot 5H_2O$, 0.16 g of $CuSO_4 \cdot 5H_2O$, and 0.11 g of $(NH_4)_6Mo_7O_{24} \cdot 4H_2O$ dissolved in 100 mL of distilled water, and the pH was adjusted to 6.5. All *Escherichia coli* strains were culture in LB media with carbenicillin antibiotic. Yeast strains were culture in YPD media (yeast extract 1%, peptone 2%, glucose 2%) at 220 rpm, 28 ºC/15 ºC.

2. **Heterologous expression of the gene cluster in *A. nidulans***

To prepare protoplasts, *A. nidulans* A1145 ΔSTΔEM was grown Oatmeal agar plates supplemented with 10 mM of uridine, 5 mM of uracil, 0.5 μg/mL of pyridoxine HCl and 2.5 μg/mL of riboflavin at 37 °C for 4 days. Fresh spores of *A. nidulans* A1145 ΔSTΔEM were inoculated into 25 mL of liquid CD media supplemented with 10 mM of uridine, 5 mM of uracil, 0.5 μg/mL of pyridoxine HCl and 2.5 μg/mL of riboflavin in a 125 mL flask and germinated at 28 ºC 250 rpm for 16 hours. Mycelia were harvested by centrifugation at 4000 rpm for 20 min and washed with 10 mL of osmotic buffer (1.2 M of $MgSO_4$, 10 mM of sodium phosphate, pH 5.8). The mycelia were transferred into 10 mL of osmotic buffer containing 30 mg of lysing enzymes from *Trichoderma* and 20 mg of Yatalase in a 125 mL flask. The cells were digested for 5 hours at 37 °C, 80 rpm. Cells were harvested in a 50 mL falcon tube and gently overlaid with 10 mL of trapping buffer (0.6 M of sorbitol, 0.1 M of Tris-HCl, pH 7.0). The cells were then centrifuged at 4300 rpm for 30 min at 4°C, the protoplasts were collected at the interface of the two buffers. The protoplasts were transferred to a sterile 15 mL falcon tube and washed with 3 volumes of STC buffer (1.2 M of sorbitol, 10 mM of $CaCl_2$, 10 mM of Tris-HCl, pH 7.5). After centrifugation at 4300 rpm, 20 min at 4 °C, the supernatant was discarded, and the protoplast pellet was resuspended in 1 mL of STC buffer.

For each transformation, 3 μL of each plasmid (>100 ng/μL) was added to 60 μL of the *A. nidulans* A1145 ΔSTΔEM protoplast suspension prepared as above, and the mixture was incubated for 1 hour on ice. 600 μL PEG solution (60% PEG, 50 mM of $CaCl_2$, and 50 mM of Tris-HCl, pH 7.5) was added to the protoplast mixture, followed by additional incubation at room temperature for 20 min. The mixture was spread on the CD sorbitol plate (CD solid medium with 1.2 M sorbitol and the appropriate supplements: 10 mM of uridine, 5 mM of uracil, 0.5 μg/mL of pyridoxine HCl, and/or 2.5 μg/mL of riboflavin according to the markers in the transformed plasmids) and incubated at 37 °C for 3-4 days.[1]

Supplementary Tables

Table S1. Primers used in this study.

Primer Name	Sequence (5'→3')
HRPKS-F-ADH2P	caactatcaactattaactatatcgtaatatgcaagcgccagcaccatcaagagacg
HRPKS-R-ADH2T	catacttgataatgaaaactataaatcgctagttcaatttcaccaaagtagacatggatg
Ma_OvaB-F-ADH2p	tatcaactattaactatatcgtaataccatatgaaactgcgtgtcgcaaacttc
NRPKS-R-Spg5t	ggtaatagcgcgatgaaacaacgtctttgcctaccctaccgccgcaatgactg
jb SPG5t F	gcaaagacgttgtttcatcgc
spg5t-R	gcttattttctgccgaattttcatgaagtttttatg
Pck1p-F-spg5t	aacttcatgaaaattcggcagaaaataagcataggaaaaaaccgagcttcctttcatcc
PCK1p R	gttgttattttattatggaataattagttgcgtg
ACPTE-F-PCK1p	caactaattattccataataaaataacaacatggccgtcaccgtgtggcaag
ACPTE-R	tcatgactggctcactcgctg
CsPT477t1-F-ADH2P	aactatcaactattaactatatcgtaatacatgtctgctggctctgaccaaattg
CsPT477t-R-SPG5t	ggtaatagcgcgatgaaacaacgtctttgcttaaataaatacgtagacgaaatactcggc
jb SPG5t F	gcaaagacgttgtttcatcgc
spg5t-R	gcttattttctgccgaattttcatgaagtttttatg
proATHCAS-F-PCK1p	caactaattattccataataaaataacaacatgattttcgatgggaccacgatgtc
proAtrunTHCAS-R-CYC1	aatgtaagcgtgacataactaattacatgagtgatgatgaggggcaaaggc
XW55-F-1-cyc1t	tcatgtaattagttatgtcacgcttacattcac
CYC1-R	gcaaattaaagccttcgagcgtcc
TEF1-F-cyc1	gttttgggacgctcgaaggctttaatttgcccgcgaatccttacatcacacc
TEF1p R	tttgtaattaaaacttagattagattgctatgc
Npga-F-TEF1	tagcaatctaatctaagttttaattacaaaatggtgcaagacacatcaagcg
NpgA-R-ADH2Tnew	gataatgaaaactataaatcgtgaaggcatttaggataggcaattacacaccccagtc
colA-XW55-F	actatcaactattaactatatcgtaataccatatggcacctccatcatccaaagtcactg
colA-R-spg5t	ggtaatagcgcgatgaaacaacgtctttgctcaagcggagcctttgagaacg
NphB-F-cox4	tgtagctctagatatctgcttcagggatccatgagcgaggccgctgacg
NphB-F-CyC1	aatgtaagcgtgacataactaattacatgattagtcctccagagaatcgaatgccttg
NphBopt-F-glaA	cttcatccccagcatcattacacctcagcaatgtcagaggcggctgacgtag
NphBopt-R-trpC	tgtttgatgatttcagtaacgttaagtggttaatcttccaggctatcaaacgccttcaac
trpC-F	ccacttaacgttactgaaatcatcaaacagc
trpC-R-pyroA	gagacccaacaaccatgataccaggggaagaaggattacctctaaacaagtgtacctgtg
TislaUbiA-F-POG	gcatacagaacacttcaaacaatcgcaaaaatgccttcaaagacagcgaacaag
TislaUbiA-R-pyroA	gatgagacccaacaaccatgataccaggggaatcggaactgaaacaggagtgttcc
hygr-F-CrGES	atgtctttgccactggctactccattgatcaatgggtaaaaagcctgaactcaccgcgac
hygr-R-CrGES	ttaaaagcatggagtaaagaacagagccttaacgtaattattcctttgccctcggacgag
BleoR-F-ObGES	atgccattatcttcaactcctttgataaatggtgacaactatggccaagttgaccagtgc
BleoR-R-ObGES	ttattgagtgaaaaacaatgcatcgacataattgtctactcagtcctgctcctcggccac
CJ-pYTU-colC_p1-F	attaccccgccacatagacacatctaaacaatgactctcatgccgtccaacac
CJ-pYTU-colC_p1-R	gcatatctctgcaagctctcagctg
CJ-pYTU-colC_p2-F	cgtgtatcaacagctacggtgcttc

CJ-pYTU-colC_p2-R	ggttctggtcatccttgagctctg
CJ-pYTU-colC_p3-F	ctagcagcagcactgacttgacc
CJ-pYTU-colC_p3-R	cacagtggaggacatacccgtaattttctgcagcgatgaaggcaggaaaggag
CJ-pYTP-colA-F	attaccccgccacatagacacatctaaacaatggcacctccatcatccaaagtc
CJ-pYTP-colA-R	gatgagacccaacaaccatgataccaggggcaggagtctgtttctgagcatcagag
CJ-POgpdA-F	tttgctccaggaatacatgtgagcttactg
CJ-POgpdA-R	ttttgcgattgtttgaagtgttctgtatgc
CJ-pYTR-colB-F	attaccccgccacatagacacatctaaacaatgagtgccattactgagcccaag
CJ-pYTR-colB-R	aagggtatcatcgaaagggagtcatccaatggttctgtacatgttgtctatcaggagagg
CJ-pYTU-colC_p2-F	cgtgtatcaacagctacggtgcttc

Table S2. Plasmids used in this study.

Plasmid name	**Vector**	**Genes**
pyIO01	XW02	*Ma_OvaA*
pyIO02	XW55	*Ma_OvaBC*
pyIO08	XW55	*TislaUbiA*
pyIO029	Pmd29	*tCsPT4+npgA*
pyIO030	Pmd29	*tCsPT4+npgA+THCAS*
pyIO031	Pmd29	*ColA+npgA+THCAS*
pMetarR01	pYTR	*Ma_OvaA*
pMetarU05	pYTU	*Ma_OvaBC*
pIO10	pYTP	*tCsPT4*
pIO13	pYTP	*NphB*
pIO23	pYTP	*ColA*
pYTU-colC	pYTU	*colC*
pYTP-colB	pYTP	*colB*
pYTR-colA	pYTR	*colA*

Table S3. Yeast Strains Used in This Study [2,3,4,5]

Strain	Parent	Genome modifications to parent	Reference
BY4742	S288C	*MATα his3Δ1 leu2Δ0 ura3Δ0 lys2Δ0*	Brachmann et al. (1998)
DHY214	BY4742	*SAL1^{+}CAT5(91M) MIP1(661T) MKT1(30G) RME1(INS-308A) TAO3(1493Q) HAP1 +*	Harvey et al. (2018)
JHY651	DHY214	*MATα prb1Δ pep4Δ*	Harvey et al. (2018)
JHY686	JHY651	*ADH2P:npgA:ACS1t*	Harvey et al. (2018)
S1	JHY651	*YPRCTy1–2Δ::iCas9::LEU2*	Yee et al. (2019)
S2	S1	*ura3Δ::TEF1p-CrGES-CYC1t*	Yee et al. (2019)
S3	S2	*rox1Δ::TEF1p-ERG20*(f)ObGES-CYC1t*	Yee et al. (2019)
S4	S3	*oye2Δ::TEF1p-mFPS-CYC1t*	Yee et al. (2019)
S5	S4	*erg9p truncation*	Yee et al. (2019)
S7	S5	*bts1Δ::TEF1p-IDI1-CYC1t*	Yee et al. (2019)
S11	S7	*yjl064wΔ::TEF1p-HMG2*-CYC1t*	Yee et al. (2019)
S12	S11	*ypl062wΔ::GPDp-tHMG1-ADH1t*	Yee et al. (2019)
yIO01	S12	*ura3Δ::TEF1p-Hygr-CYC1t*	*This study*
yIO02	yIO01	*rox1Δ::TEF1p-ERG20*(f)zeo-CYC1t*	*This study*

Table S4. ^{1}H (500 MHz) and ^{13}C NMR (125 MHz) for CBGPA in DMSO-d_6

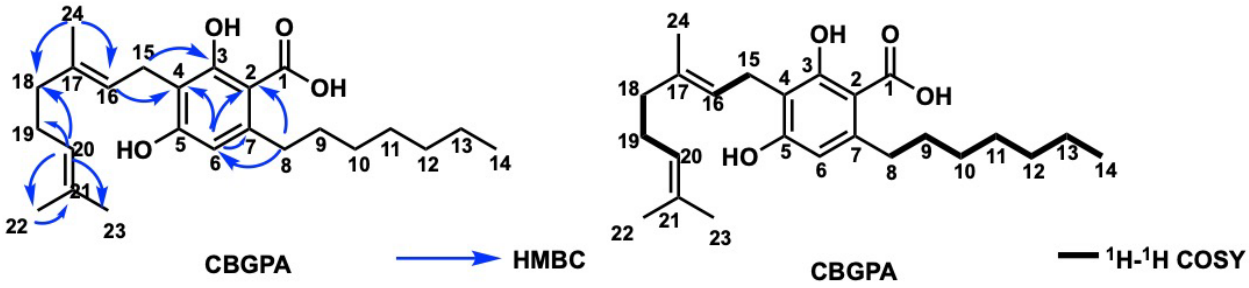

position	^{13}C	^{1}H (J in Hz)
1	173.5	-
2	144.4	-
3	163.2	-
4	111.7	-
5	155.7	-
6	109	6.13 (s, 1H)
7	106.2	-
8	35.6	2.84 (m, 2H)
9	31.6	1.52 (s, 2H)
10	31.4	1.3-1.45 (m, 8H)
11	31.3	
12	30.8	
13	29.3	
14	14	0.86 (t, 3H, 6.7)
15	21.7	3.15 (d, 2H, 7.2)
16	124.2	5.15 (m, 1H)
17	132.6	-
18	40.4	1.9 (m, 2H)
19	28.6	7.99 (q, 2H, 7.4)
20	124.3	5.03 (tq, 1H, 8.6, 1.9)
21	130.6	-
22	26.2	1.59 (m, 3H)
23	17.5	1.52 (m, 3H)
24	15.7	1.69 (m, 3H)

Table S5. ^{1}H (500 MHz) and ^{13}C NMR (125 MHz) for Δ^{9} –THCPA in DMSO-*d*$_6$

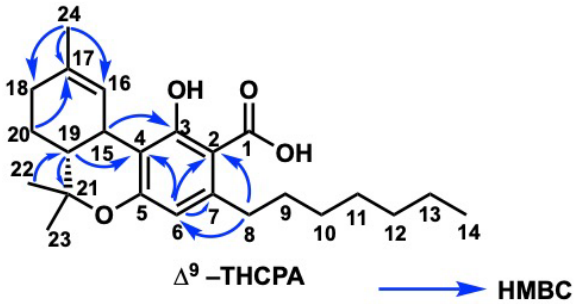

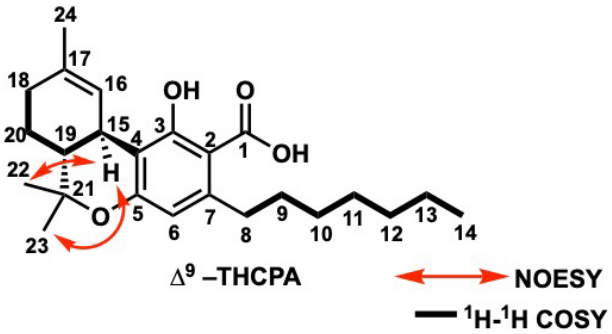

position	^{13}C	^{1}H (*J* in Hz)
1	172.2	-
2	144.6	-
3	165.6	-
4	110.1	-
5	154.2	-
6	107	5.68 (s, 1H)
7	107.9	-
8	35	1.24 (m, 12H)
9	31.6	
10	31.4	
11	29.5	
12	28.9	
13	22.2	
14	14	0.82 (t, 3H, 6.7)
15	33.5	3 (m, 1H)
16	125.3	6.49 (q, 1H, 1.7)
17	131.1	-
18	30.1	1.24 (m, 2H)
19	27.2	2.05 (m, 2H)
20	45.8	1.49 (s, 1H)
21	76.4	-
22	27.4	1.28 (s, 3H)
23	19.2	0.95 (s, 3H)
24	23.1	1.57 (d,3H, 1.8)

Table S6. ^{1}H (500 MHz) and ^{13}C NMR (125 MHz) for Δ^{9} –THCP in CD_3OD

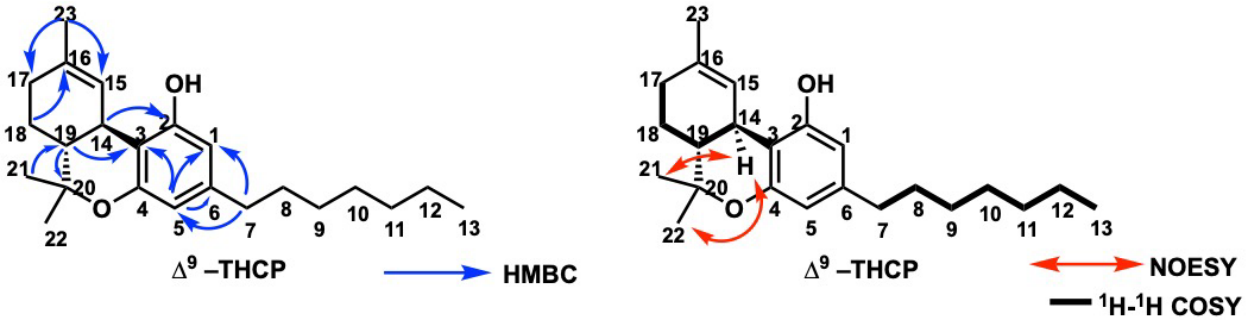

position	^{13}C	^{1}H (*J* in Hz)
1	108.4	6.16 (s, 1H, 1.8)
2	157.2	-
3	110.4	-
4	155.8	-
5	109.7	5.08 (s, 1H)
6	143.4	-
7	35.2	2.41 (m, 2H)
8	32.4	1.3 (m, 10H)
9	32.3	
10	30.6	
11	30.5	
12	23.7	
13	14.4	0.9 (td, 3H, 7.0, 2.4)
14	33	3.32 (s, 1H)
15	126.2	6.43 (m, 1H)
16	133.5	-
17	30.8	2.32 (t, 2H, 7.5)
18	26.3	1.33 (m, 2H)
19	47.5	1.62 (m, 2H)
20	77.9	-
21	28	1.37 (s, 3H)
22	19.4	1.05 (s, 3H)
23	17.1	1.66 (dd, 3H, 2.3, 1.3)

Table S7. ^{1}H (500 MHz) and ^{13}C NMR (125 MHz) for **3** in DMSO-*d*$_6$

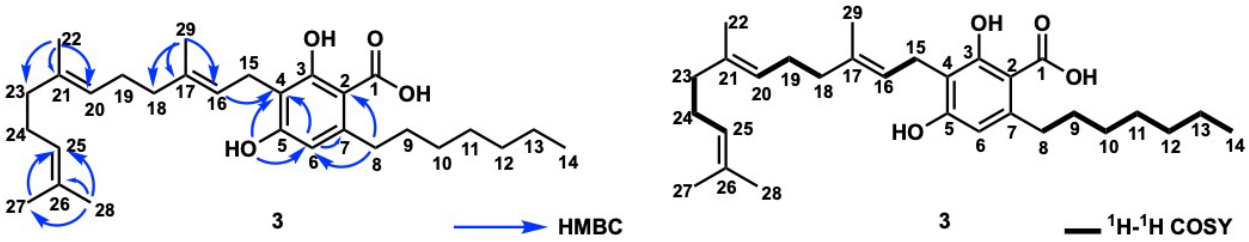

position	^{13}C	^{1}H (*J* in Hz)
1	174.5	-
2	144.4	-
3	164	-
4	112.7	-
5	158.4	-
6	109	6.14 (s, 1H)
7	106.1	-
8	34.6	2.92 (dt, 2H, 12.2, 7.5)
9	31.3	1.63 (m, 2H)
10	31.1	1.42-1.59 (m, 8H)
11	29.4	
12	29.1	
13	29	
14	14	0.85 (m, 3H)
15	21.8	3.06 (d, 2H, 7.3)
16	123.1	5.1 (m, 1H)
17	132.8	-
18	40.3	1.8 (m, 2H)
19	26.3	1.85-2 (m, 2H)
20	124.2	5.05 (m, 1H)
21	134.2	-
22	15.8	1.5 (m, 3H)
23	40.3	1.8 (m, 2H)
24	26.2	1.85-2 (m, 2H)
25	124.1	5.05 (m, 1H)
26	130.5	-
27	25.5	1.63 (m, 3H)
28	15.7	1.53 (m, 3H)
29	17.5	1.54 (m, 3H)
5-OH	-	9.42 (s, 1H)

Table S8. ^{1}H (500 MHz) and ^{13}C NMR (125 MHz) for CBGCA in CD_3OD

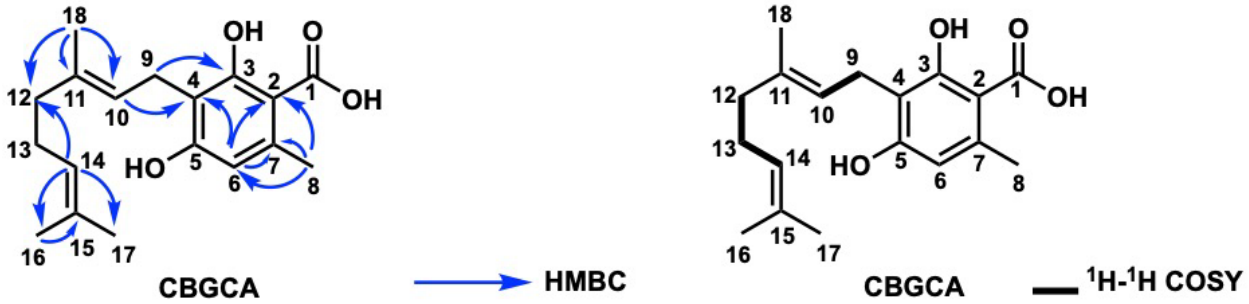

position	^{13}C	^{1}H (*J* in Hz)
1	ND	-
2	141.7	-
3	164.3	-
4	113.7	-
5	160.5	-
6	111.1	6.17 (s, 1H)
7	106.6	-
8	24.2	2.47 (s, 3H)
9	22.8	3.26 (d, 2H, 7.1)
10	124.1	5.21 (tt, 1H, 5.9, 3.1)
11	134.9	-
12	41	1.94 (dd, 2H, 8.3, 6.7)
13	27.8	2.05 (m, 2H)
14	125.5	5.06 (tdt, 1H, 5.8, 3.0,1.5)
15	132	-
16	25.9	1.62 (m, 3H)
17	17.7	1.52 (m, 3H)
18	16.2	1.75 (d, 3H, 1.3)

ND: The carbon signal was not detected.

Table S9. ^{1}H (500 MHz) and ^{13}C NMR (125 MHz) for Δ^{9}–THCCA in CD_3OD

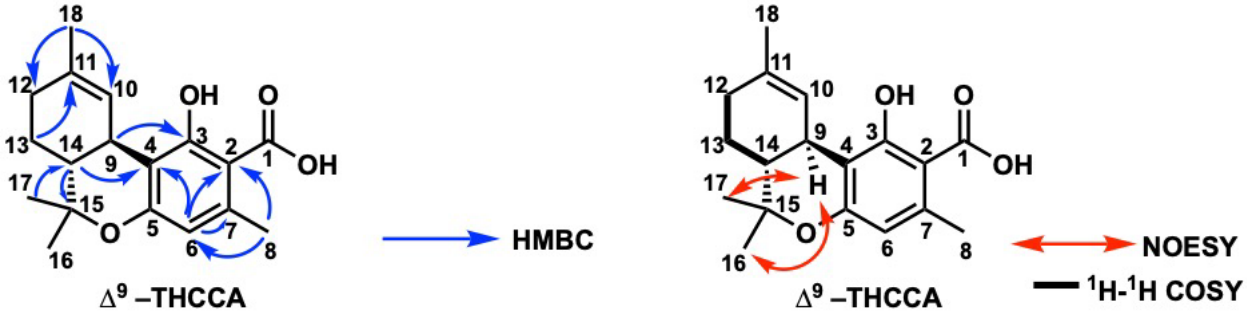

position	^{13}C	^{1}H (J in Hz)
1	ND	-
2	141.1	-
3	163.4	-
4	112.1	-
5	157.1	-
6	109	6.09 (s, 1H)
7	111.3	-
8	22.6	2.48 (m, 3H)
9	33.7	3.17 (m, 1H)
10	124.2	6.43 (dt, 1H, 8.4, 1.7)
11	132.3	-
12	30.9	2.11 (d, 2H, 7.8)
13	24.8	1.95 (m, 2H)
14	45.9	1.55 (m, 1H)
15	77.5	-
16	26.4	1.41 (m, 3H)
17	18.2	1.05 (m, 3H)
18	22.1	1.6 (m, 3H)

ND: The carbon signal was not detected.

Supplementary Figures

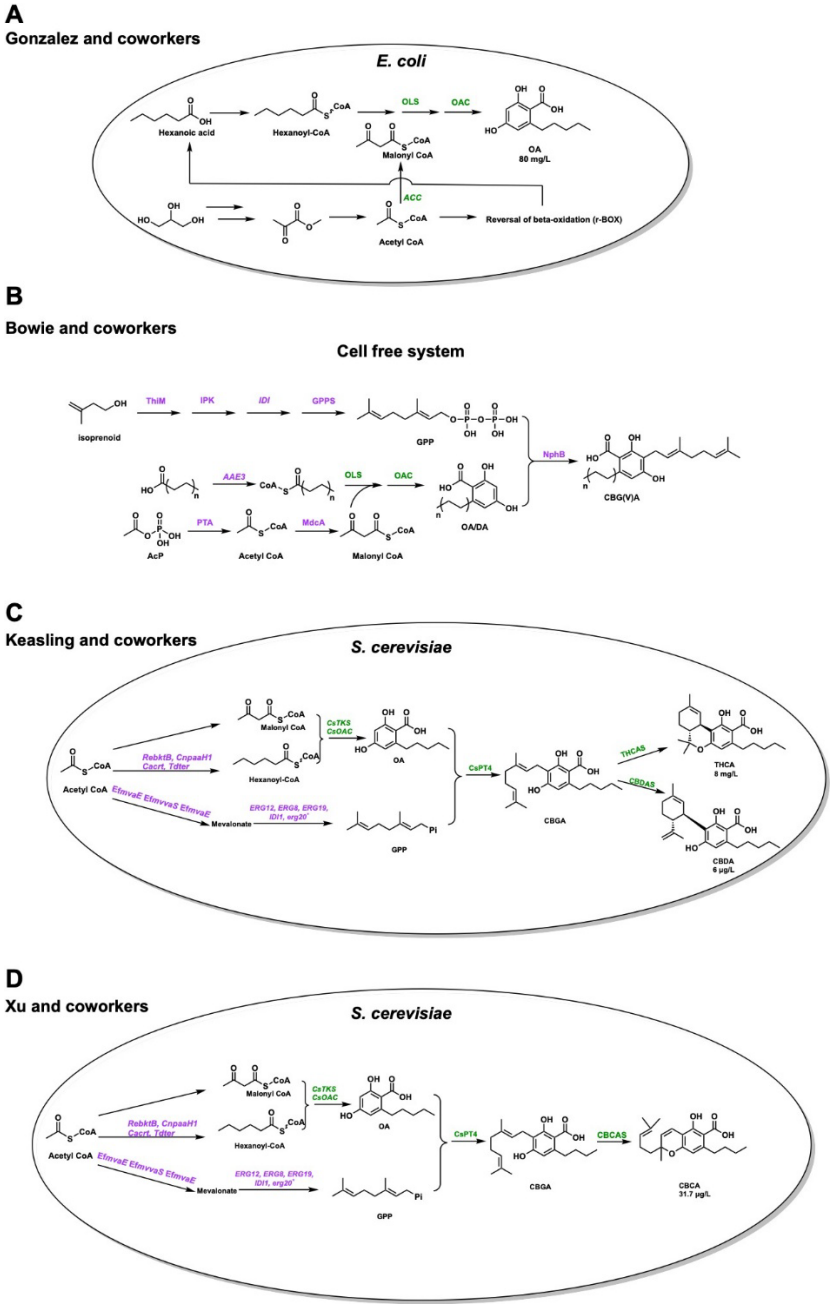

Figure S1. Previous work on microbial production of cannabinoids. A) Gonzalez and co-workers integrated OA biosynthesizing pathway in *E. coli* and achieved 80 mg/L OA production. B) The cell free system designed by Bowie and coworkers relies on *in vitro* reactions to produce CBGA and CBGVA. D) Keasling and co-workers fully integrate the plant pathway in yeast and after engineering the yeast strain, they achieved 8 mg/L Δ^9-THCA production and 4.8 mg/L Δ^9-THCVA production. E) Xu and co-workers also integrated the plant pathway into yeast, and by engineering the yeast strain and expressing CBCAS, they achieved 31.7 µg/L CBCA production.

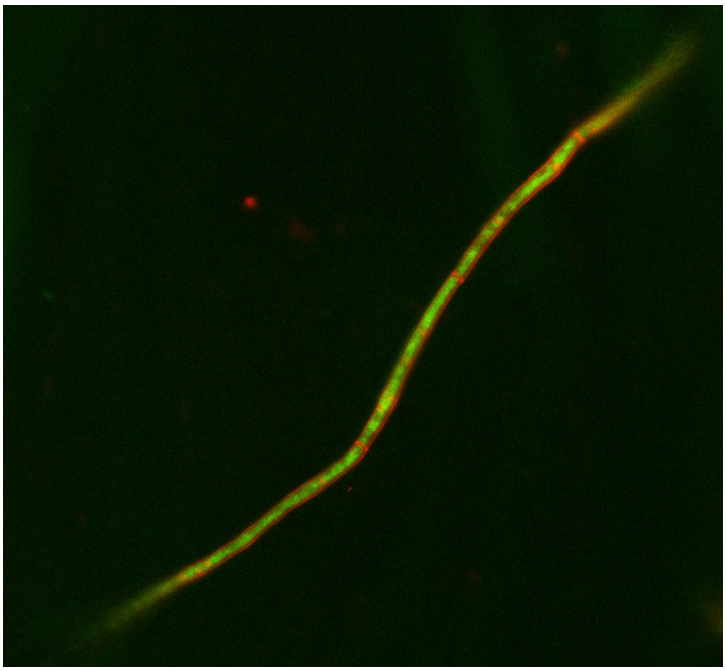

Figure S2. Localization assays of NphB in *A. nidulans*. (146 x 146 μm). The NphBM31s is fused with enhanced green fluorescent protein (EGFP) and stained with Hoescht. The red dots are nucleus. The green signal is from the EGFP fused with NphB. In terms of the picture, the green signal is separated from the nucleus, so the NphB is localized in the cytoplasm.

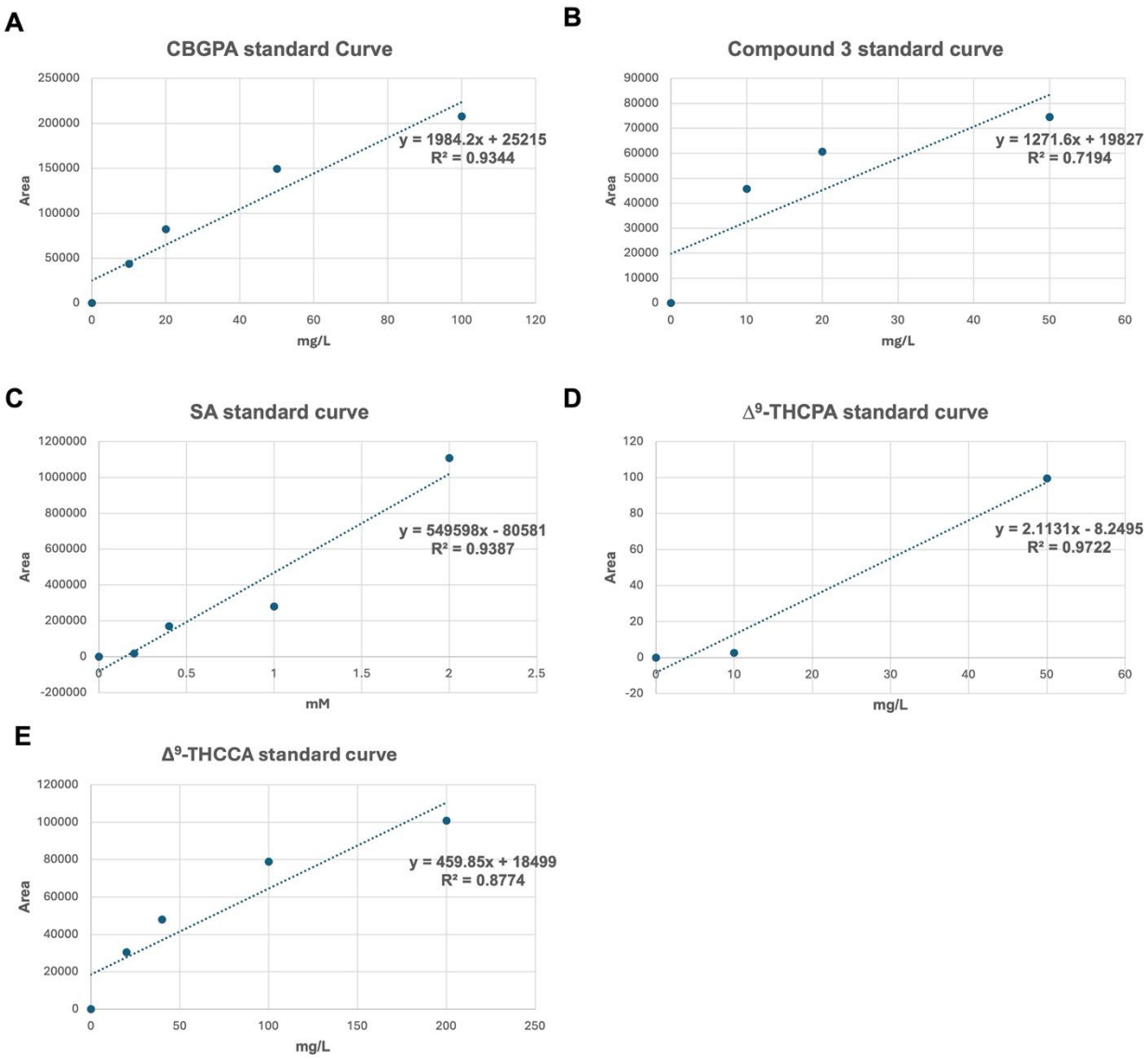

Figure S3. Standard curves of CBGPA, shunt product **3**, SA, Δ^9-THCPA, and Δ^9-THCCA. Different concentrations of purified compounds were measured on the HPLC where the area under the peak was recorded and plotted with the concentrations.

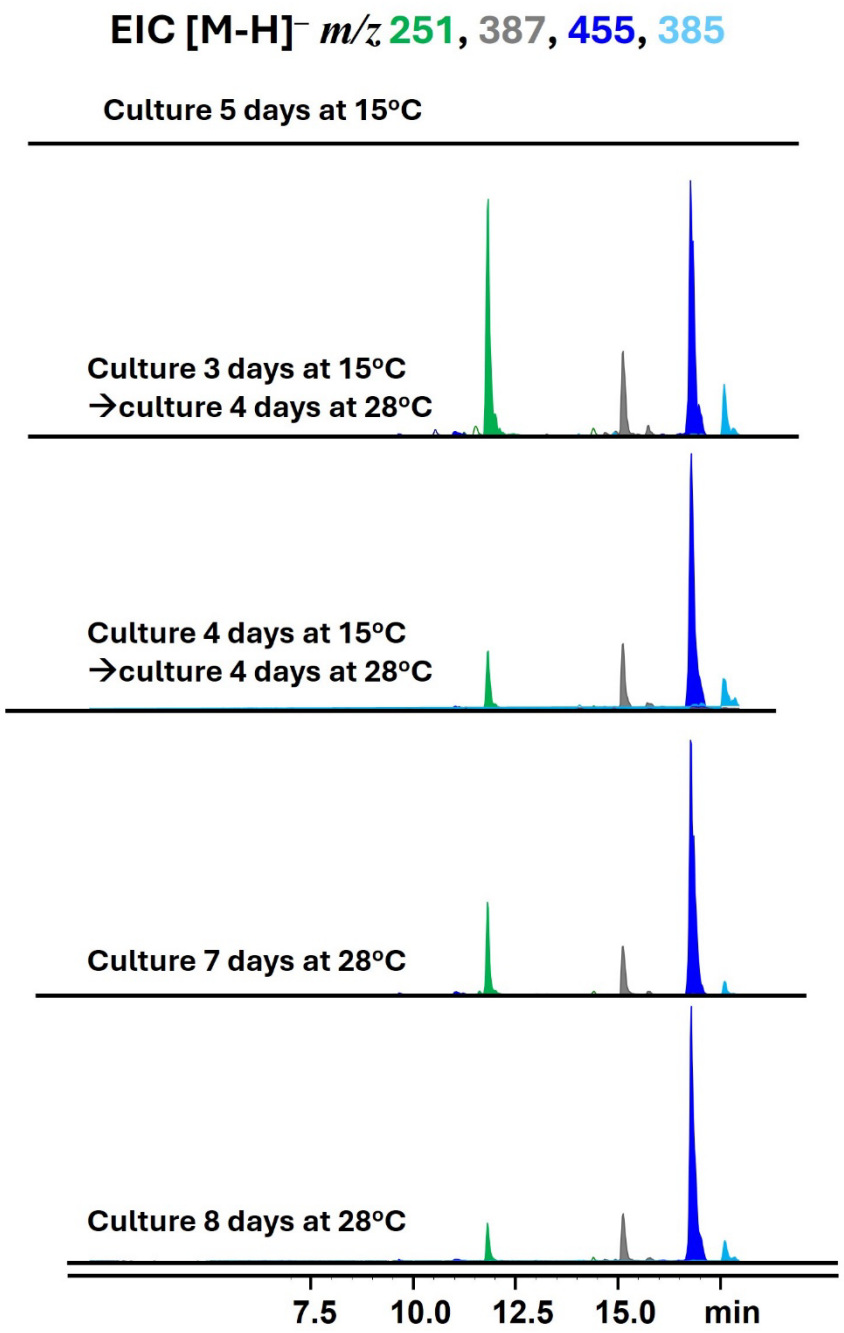

Figure S4. Metabolite analysis of yIO02 transformant at different temperatures. Metabolites profile of yeast transformants expressing Ma_OvaABC + tCSPT4 + NpgA + THCAS. The optimal condition is culturing at 15°C for 3 days and then shifting to 28°C and culture for 4 days. Fermentation at 15 °C did not produce any products.

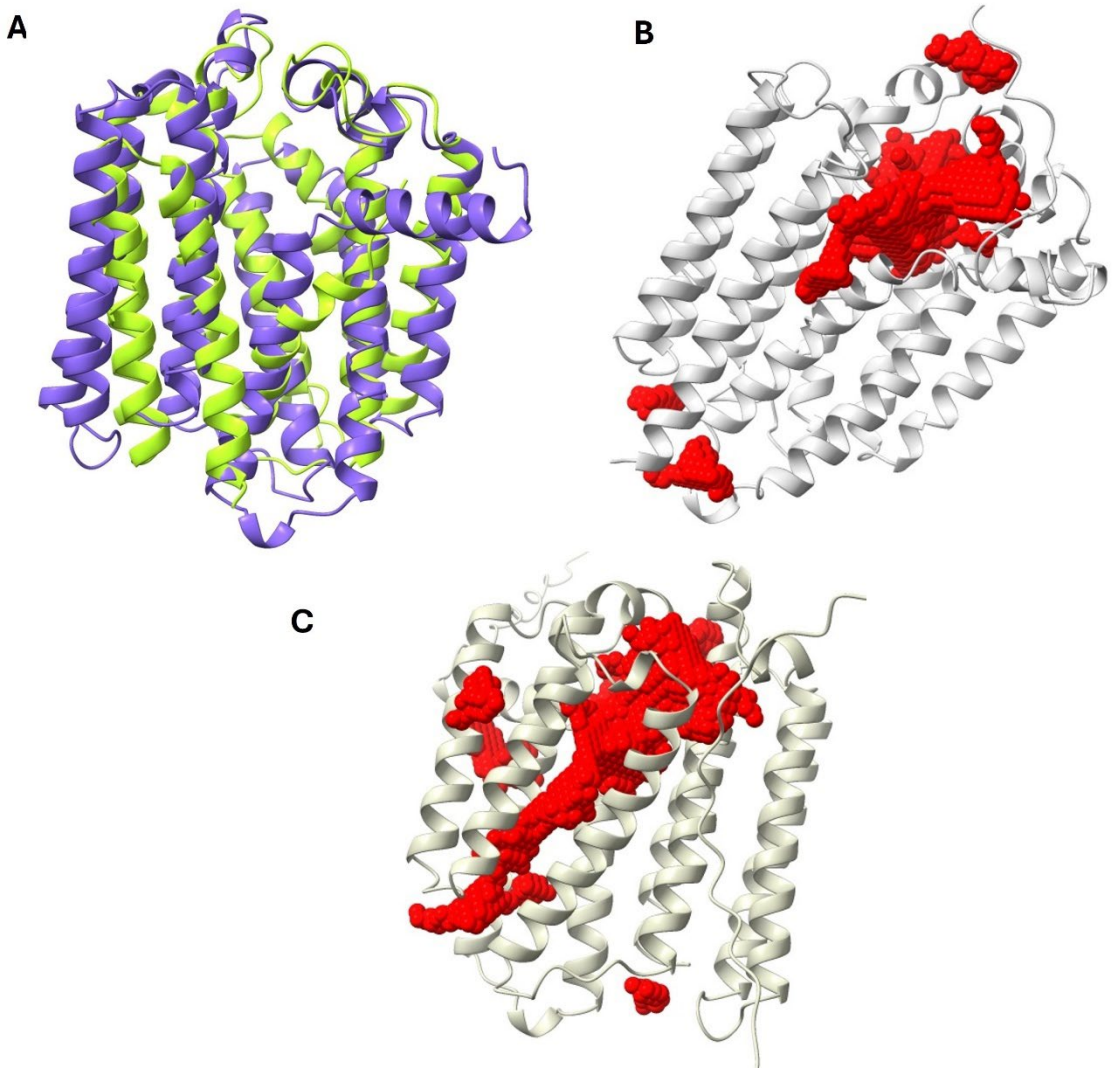

Figure S5. The structural comparison between three UbiA-prenyltransferases, 4OD4, CsPT4 and ColA. A) The structural alignment between crystal structure of 4OD4 (green) and the Alphafold predicted structure of CsPT4 (blue). The two structures align well overall. CsPT4 exhibits bigger central cavity obtaining substrates. B) The predicted binding pocket (red) of ColA. The binding pocket of ColA is smaller which limits the enzyme to accept substrates with long alkyl chains. C) The predicted binding pocket (red) of CsPT4. Similar to 4OD4, the binding pocket of CsPT4 has an unrestricted hydrophobic wall which makes the enzyme non-selective to substrates with various lengths of alkyl chain.[6,7]

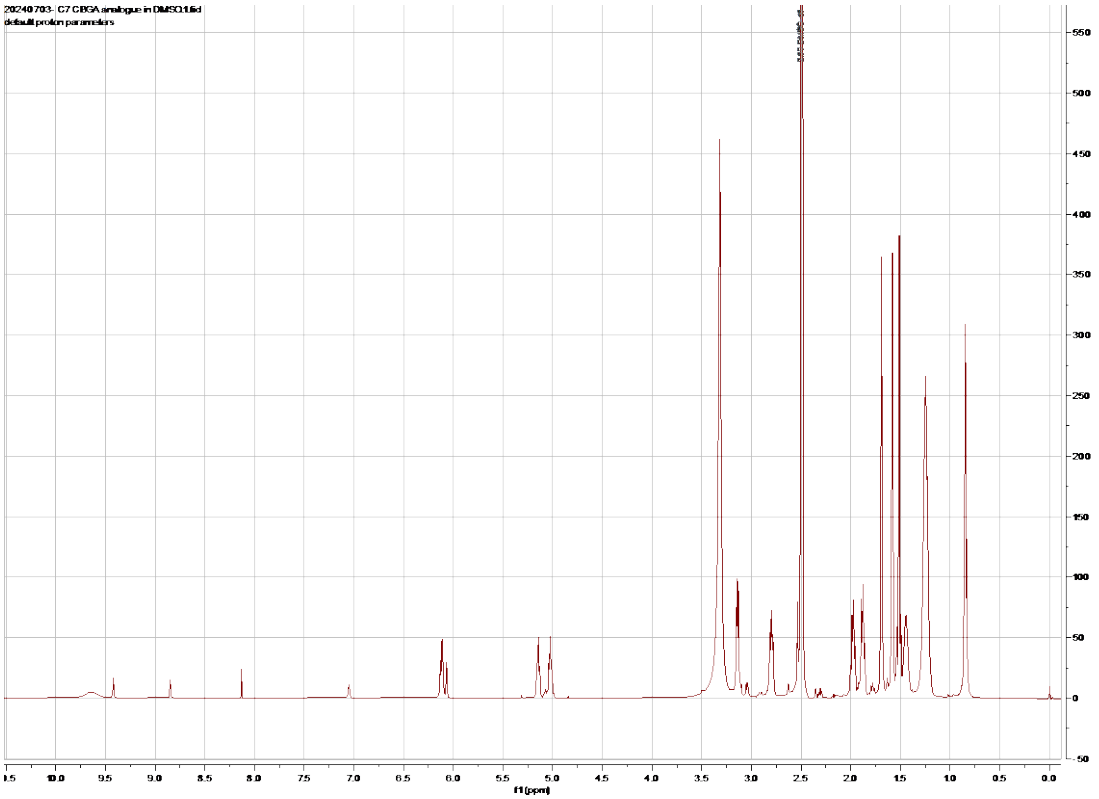

Figure S6 ^{1}H NMR spectrum of compound CBGPA in DMSO-*d*$_6$ (500 MHz)

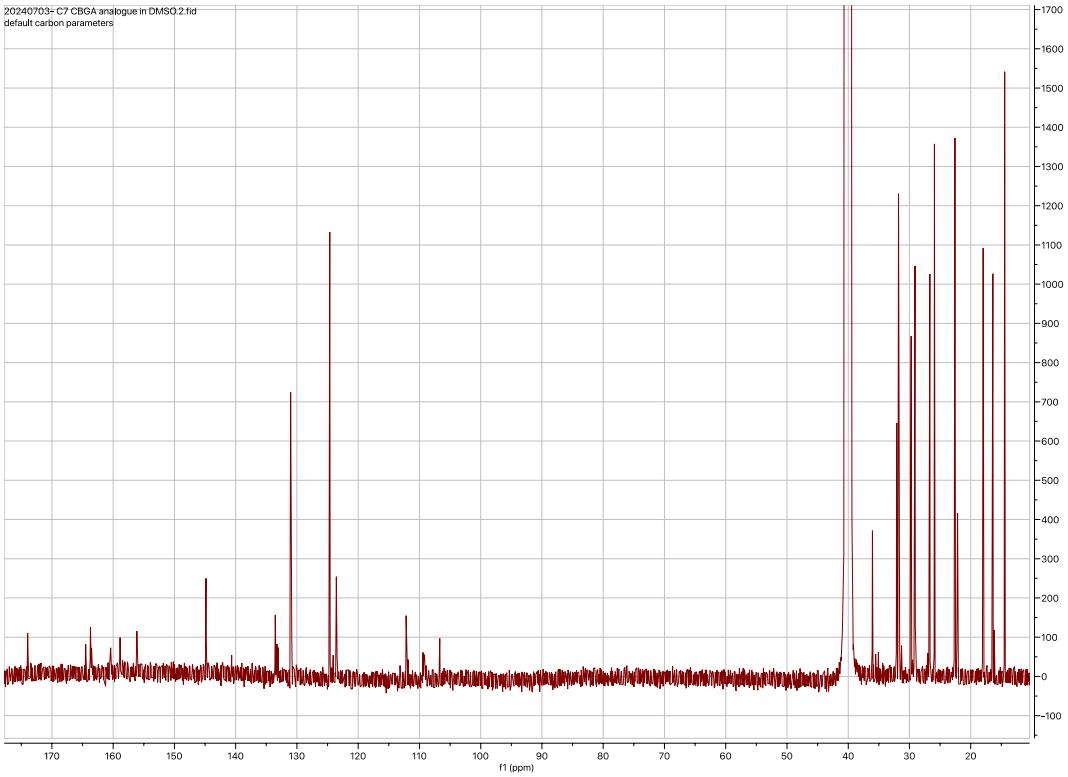

Figure S7 ^{13}C NMR spectrum of compound CBGPA in DMSO-*d*$_6$ (125 MHz)

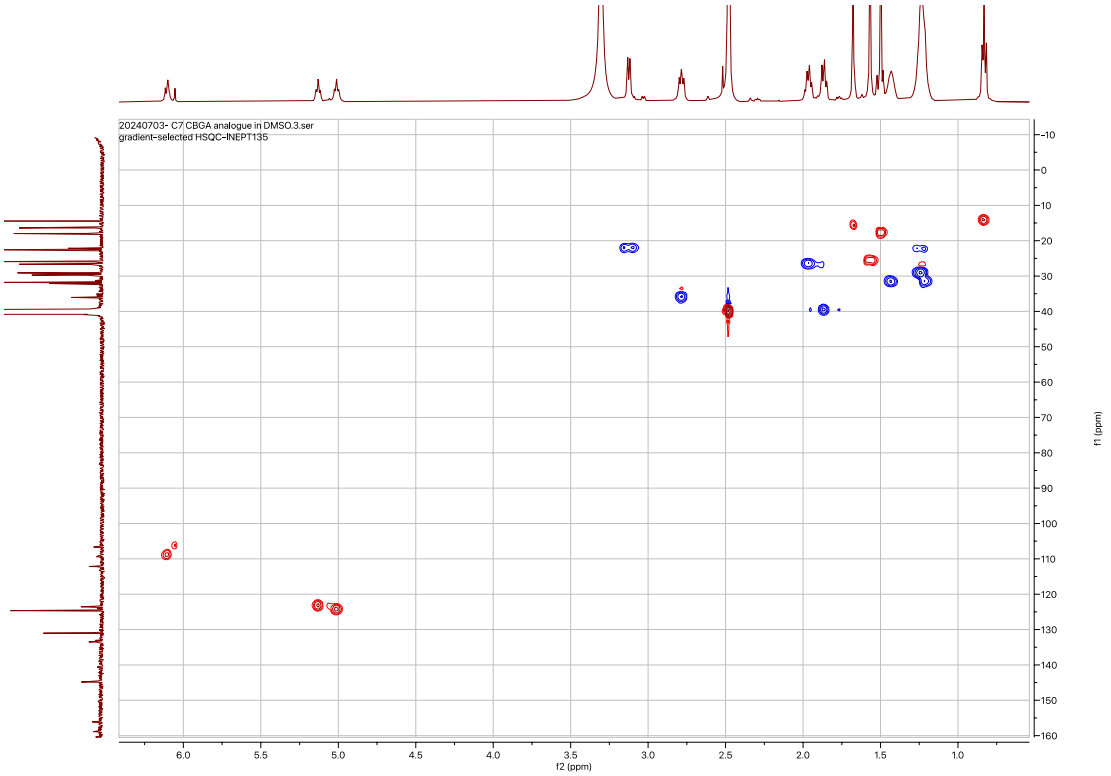

Figure S8 ^{1}H-^{13}C HSQC spectrum of compound CBGPA in DMSO-*d*$_6$ (500 MHz)

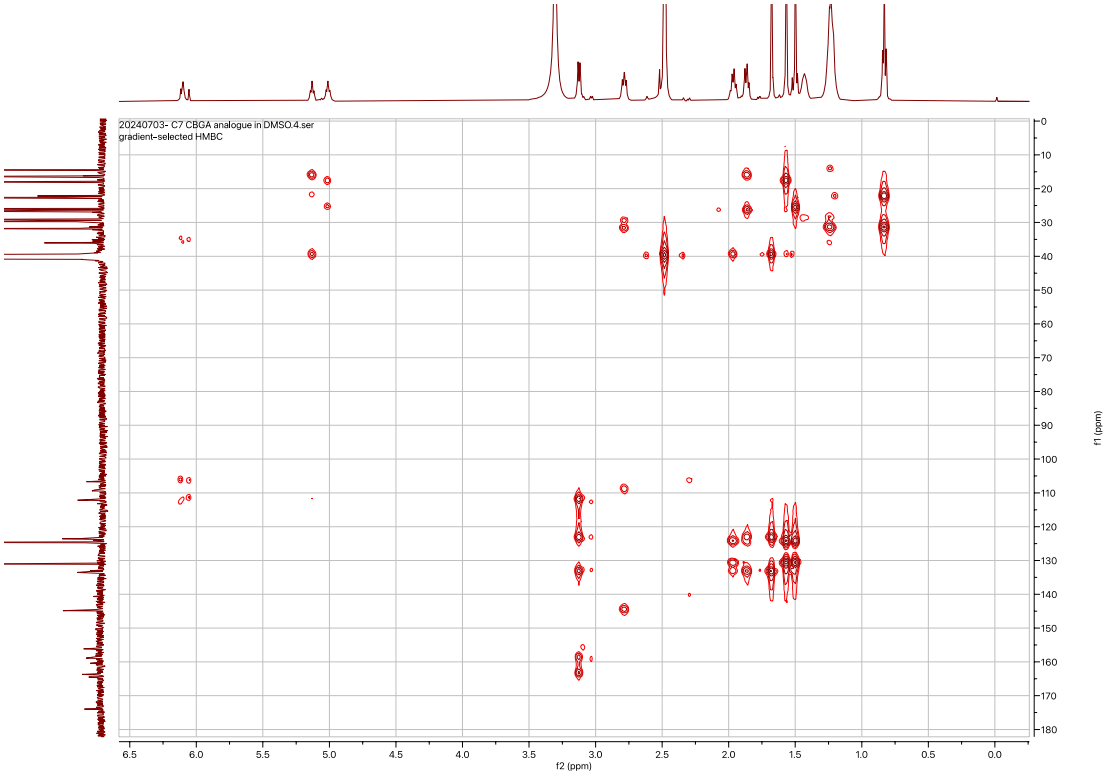

Figure S9 ^{1}H-^{13}C HMBC spectrum of compound CBGPA in DMSO-*d*$_6$ (500 MHz)

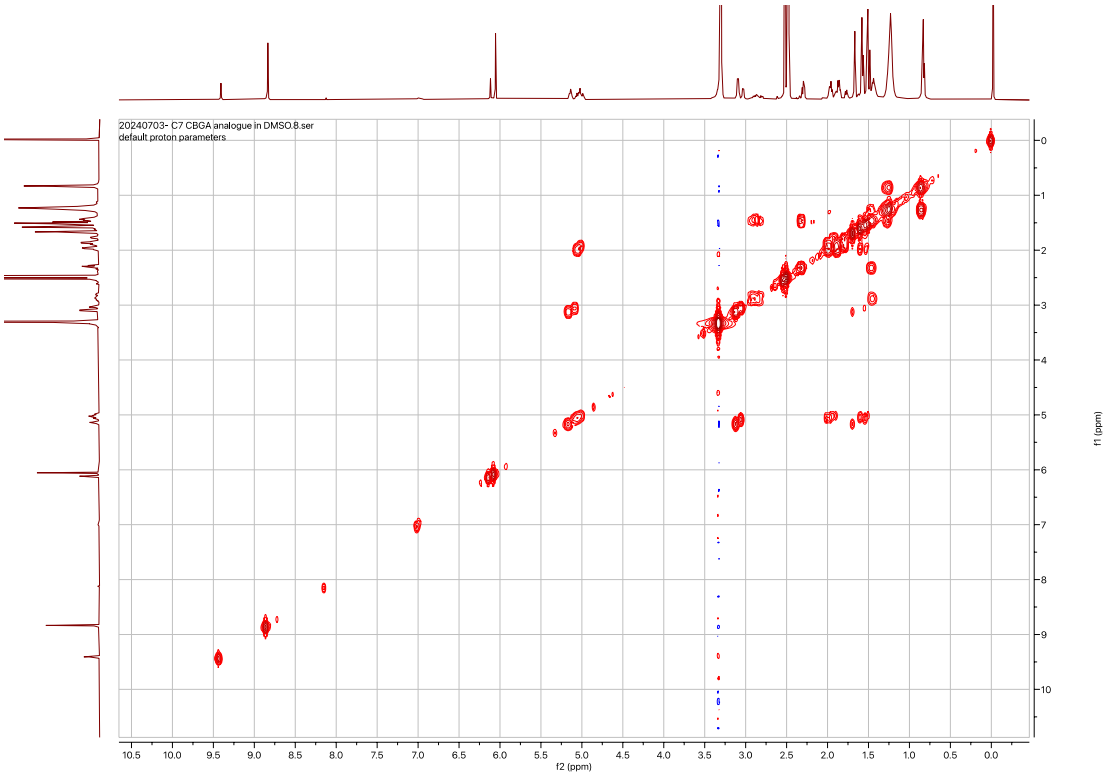

Figure S10 ^{1}H-^{1}H COSY spectrum of compound CBGPA in DMSO- *d*$_6$ (500 MHz)

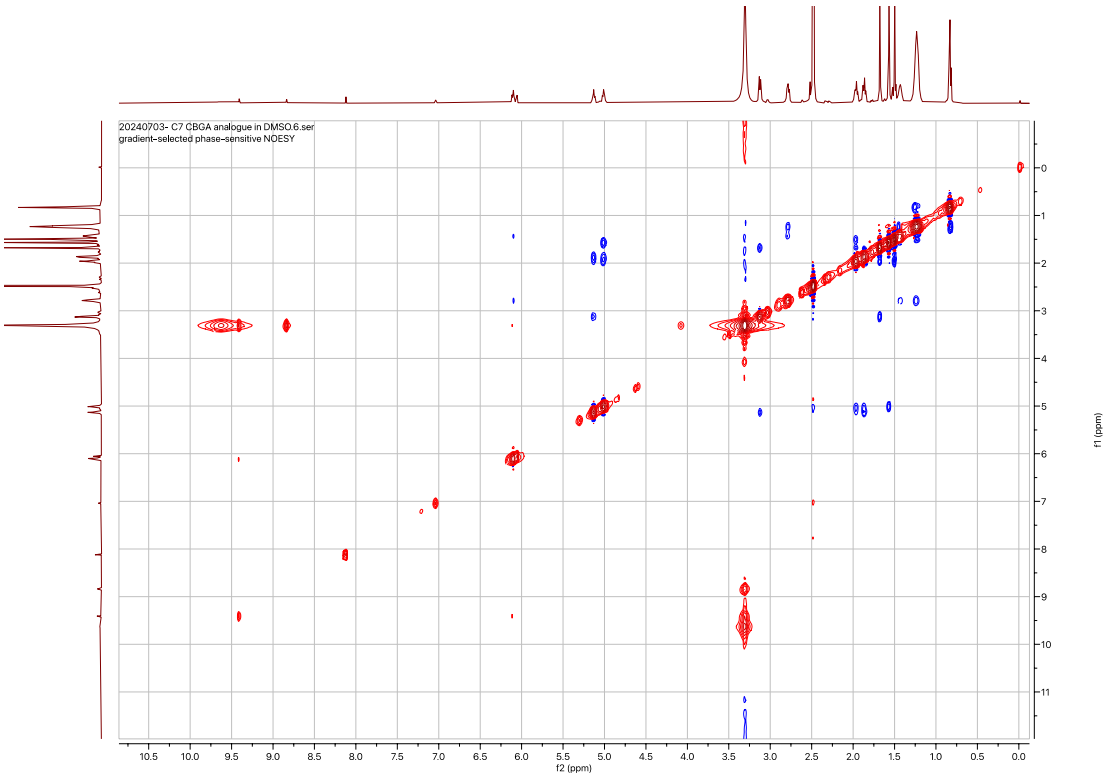

Figure S11 ^{1}H-^{1}H NOESY spectrum of compound CBGPA in DMSO-*d*$_6$ (500 MHz)

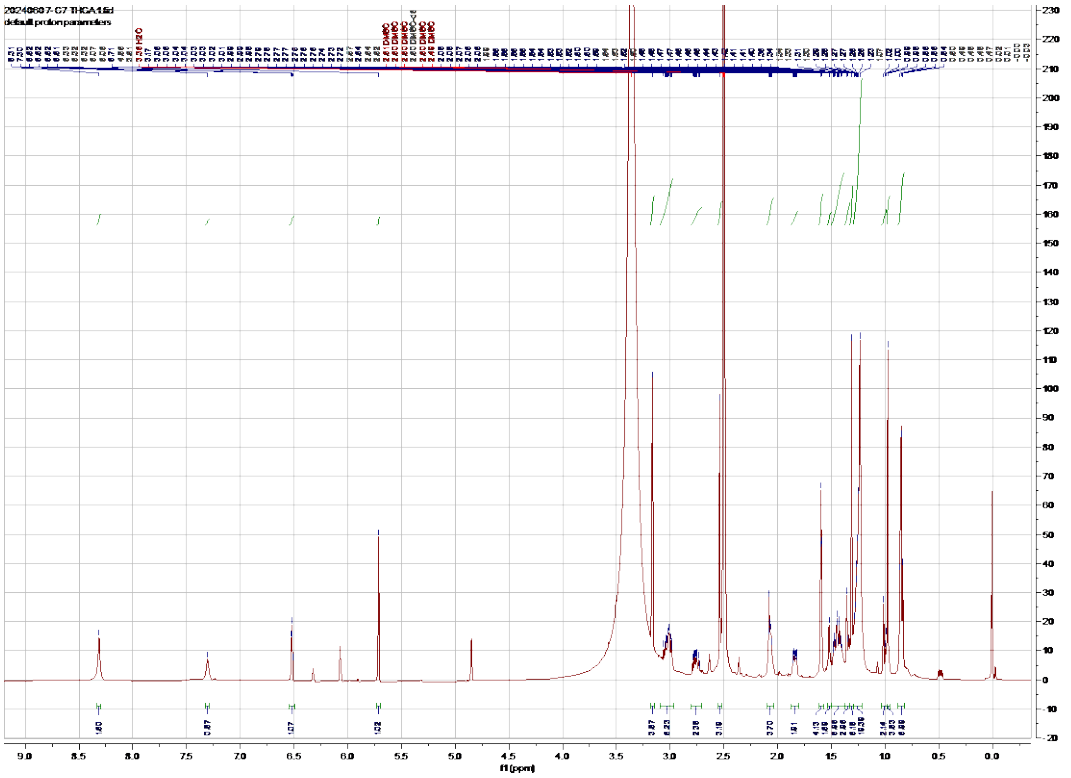

Figure S12 ^{1}H NMR spectrum of compound Δ^{9} –THCPA in DMSO-*d*$_{6}$ (500 MHz)

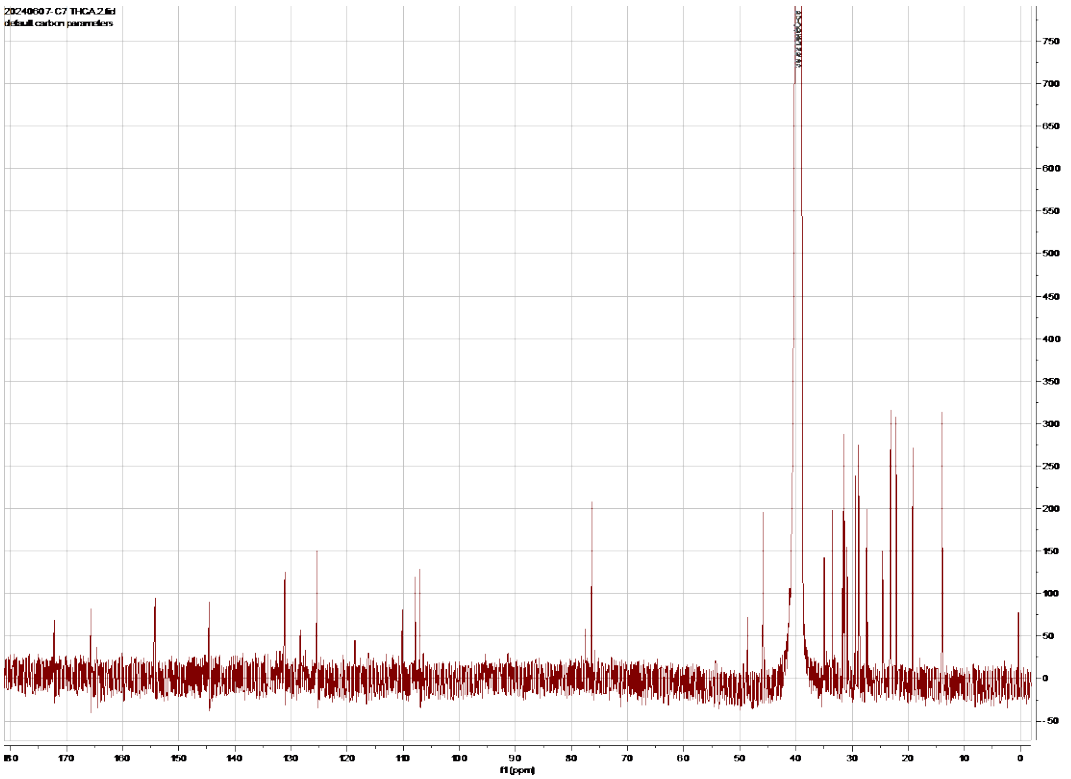

Figure S13 ^{13}C NMR spectrum of compound Δ^{9} –THCPA in DMSO-*d*$_{6}$ (125 MHz)

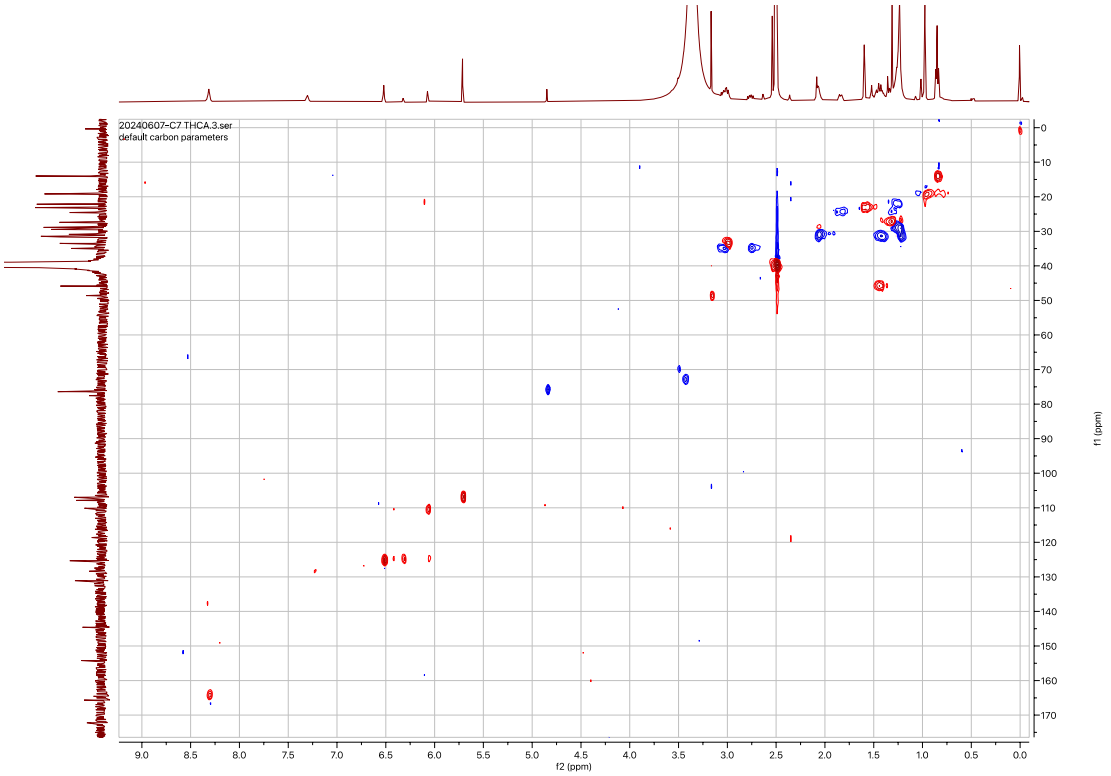

Figure S14 ^{1}H-^{13}C HSQC spectrum of compound Δ^{9} –THCPA in DMSO-*d*$_6$ (500 MHz)

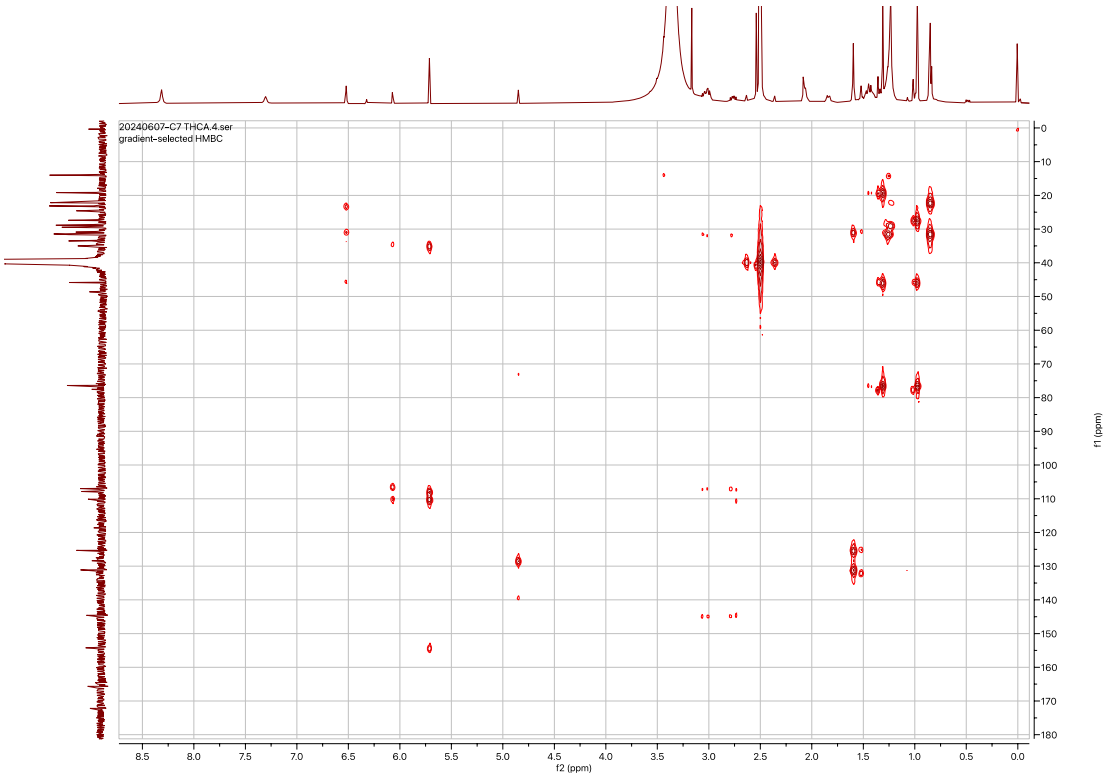

Figure S15 ^{1}H-^{13}C HMBC spectrum of compound Δ^{9} –THCPA in DMSO-*d*$_6$ (500 MHz)

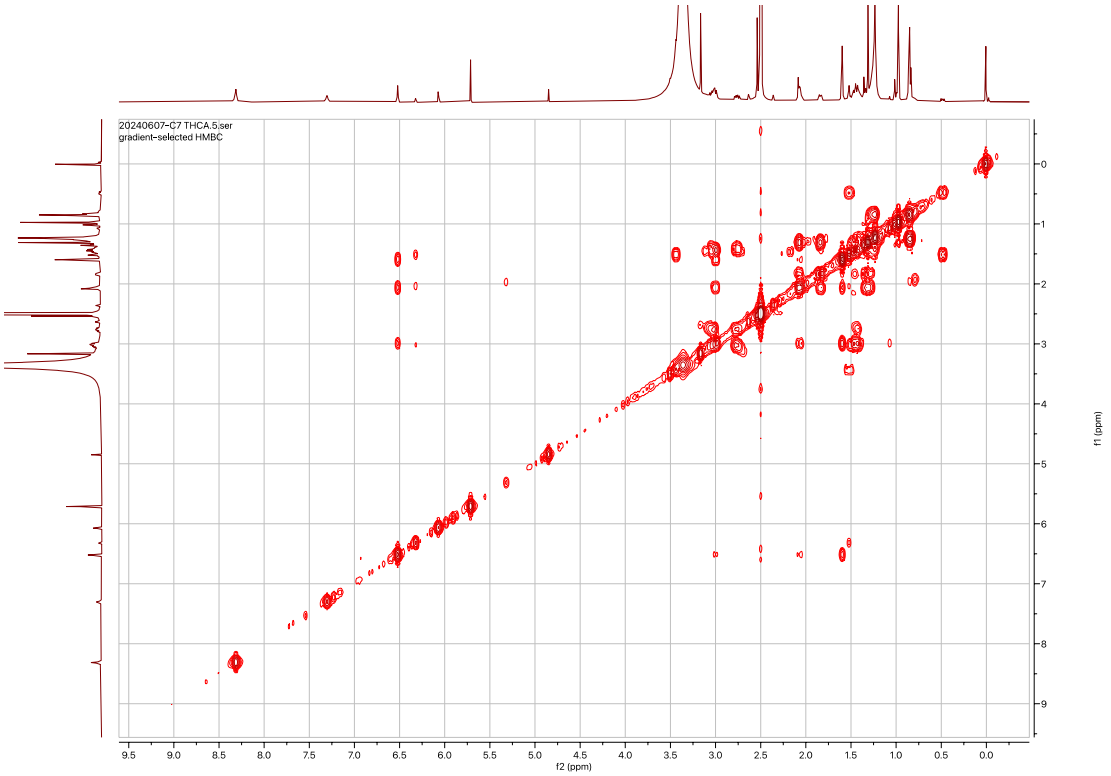

Figure S16 ^{1}H-^{1}H COSY spectrum of compound Δ^{9} –THCPA in DMSO-*d*$_{6}$ (500 MHz)

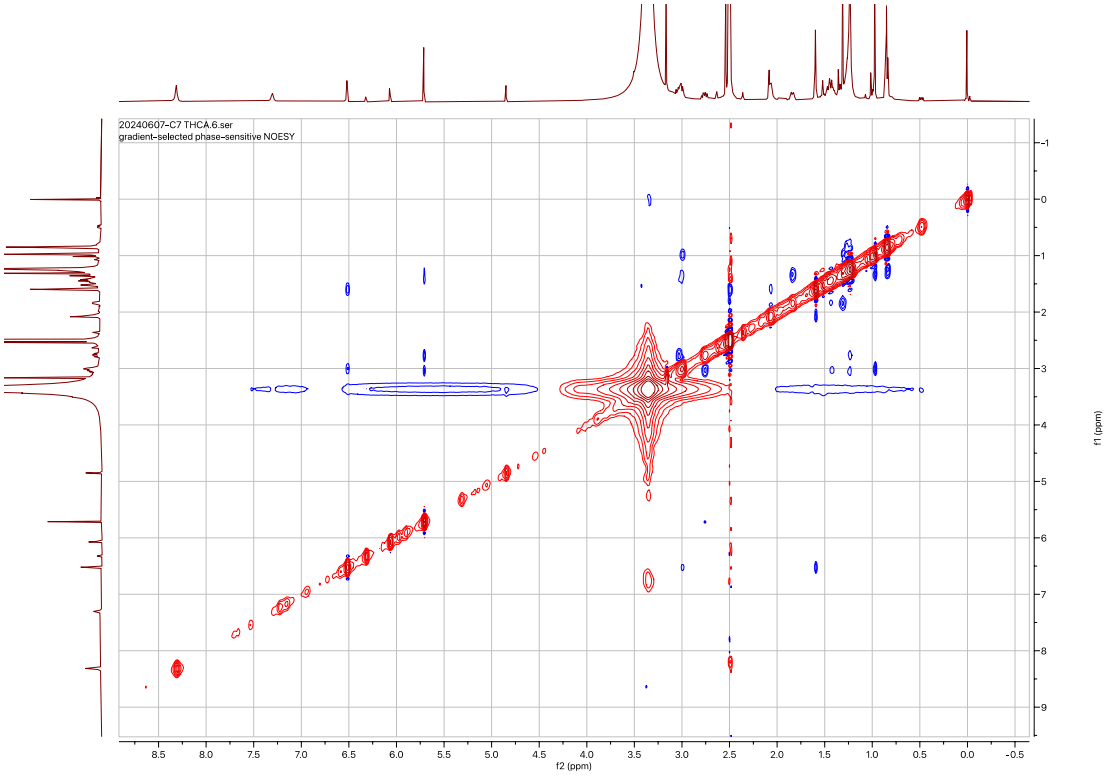

Figure S17 ^{1}H-^{1}H NOESY spectrum of compound Δ^{9} –THCPA in DMSO-*d*$_{6}$ (500 MHz)

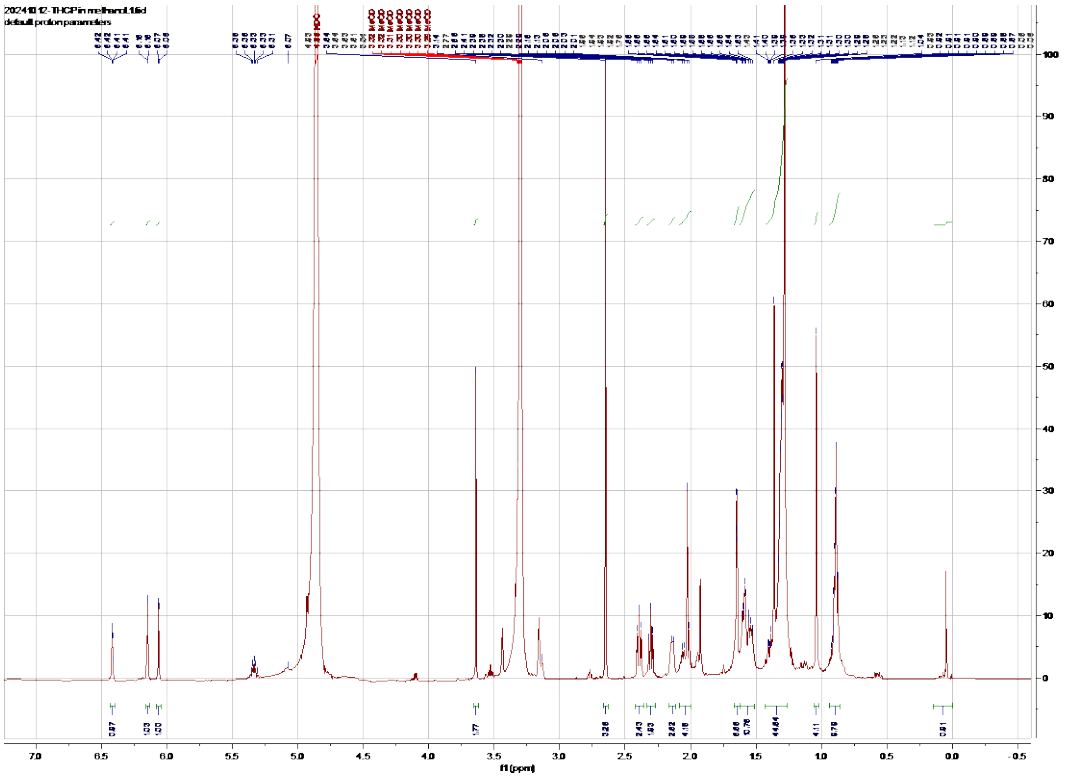

Figure S18 ^{1}H NMR spectrum of compound Δ^{9} –THCP in CD_3OD (500 MHz)

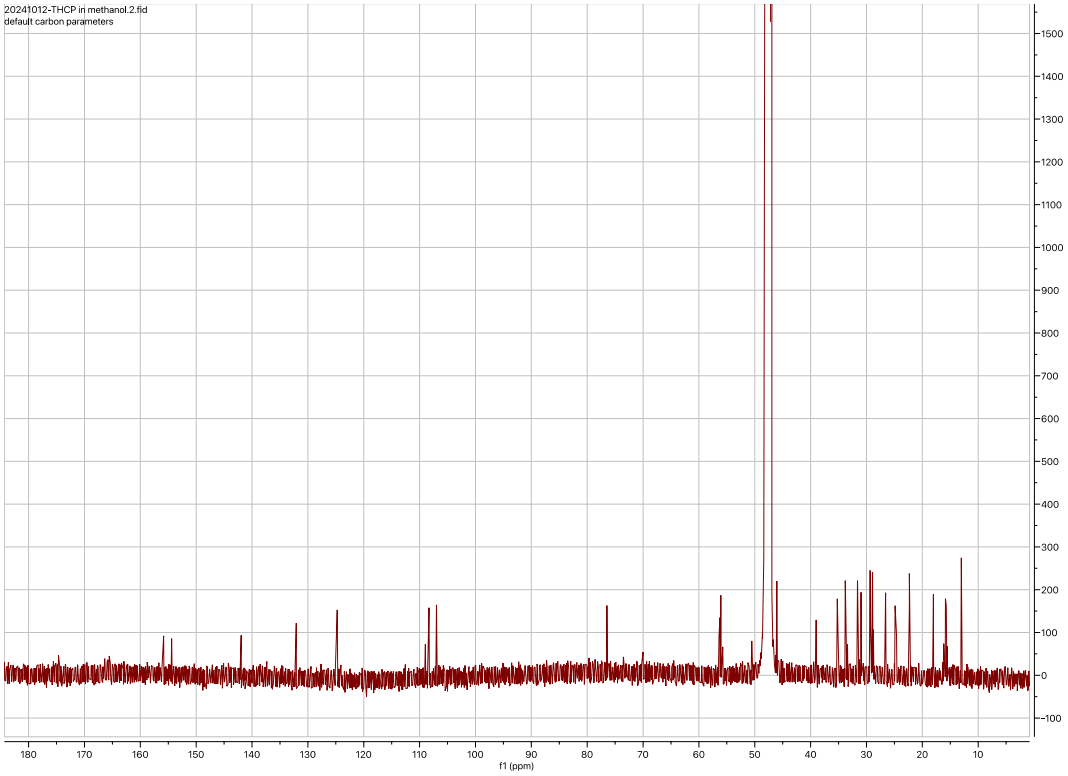

Figure S19 ^{13}C NMR spectrum of compound Δ^{9} –THCP in CD_3OD (125 MHz)

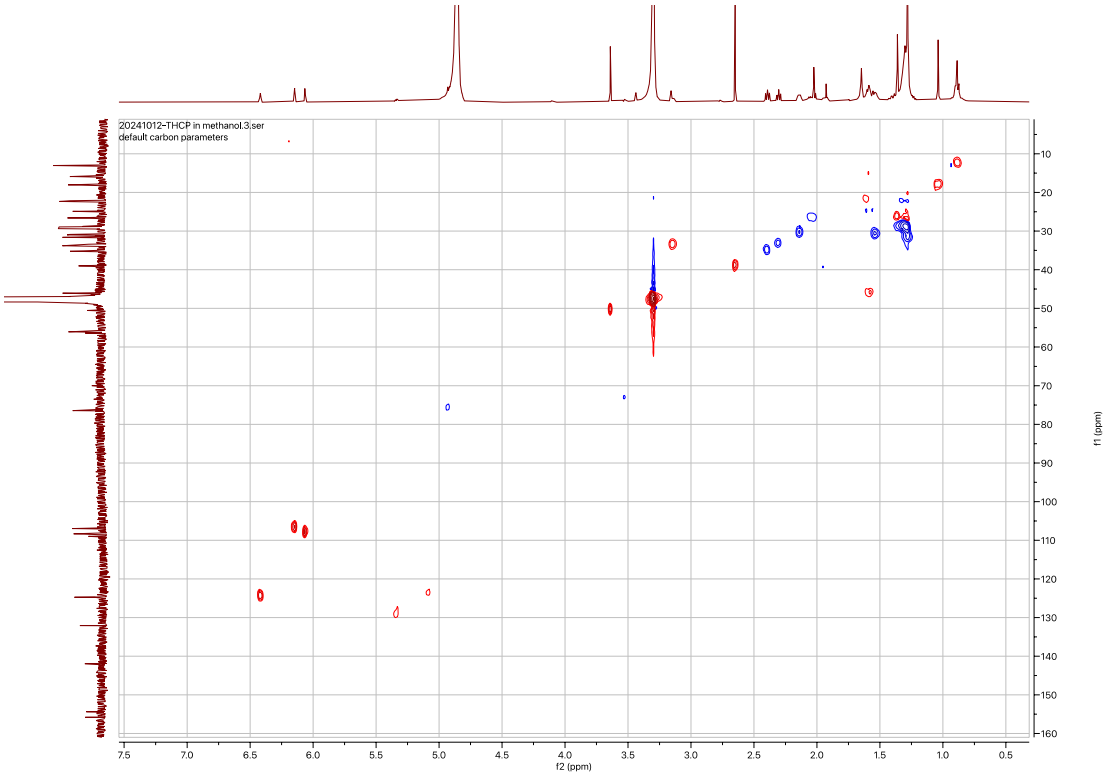

Figure S20 ^{1}H-^{13}C HSQC spectrum of compound Δ^{9} –THCP in CD_3OD (500 MHz)

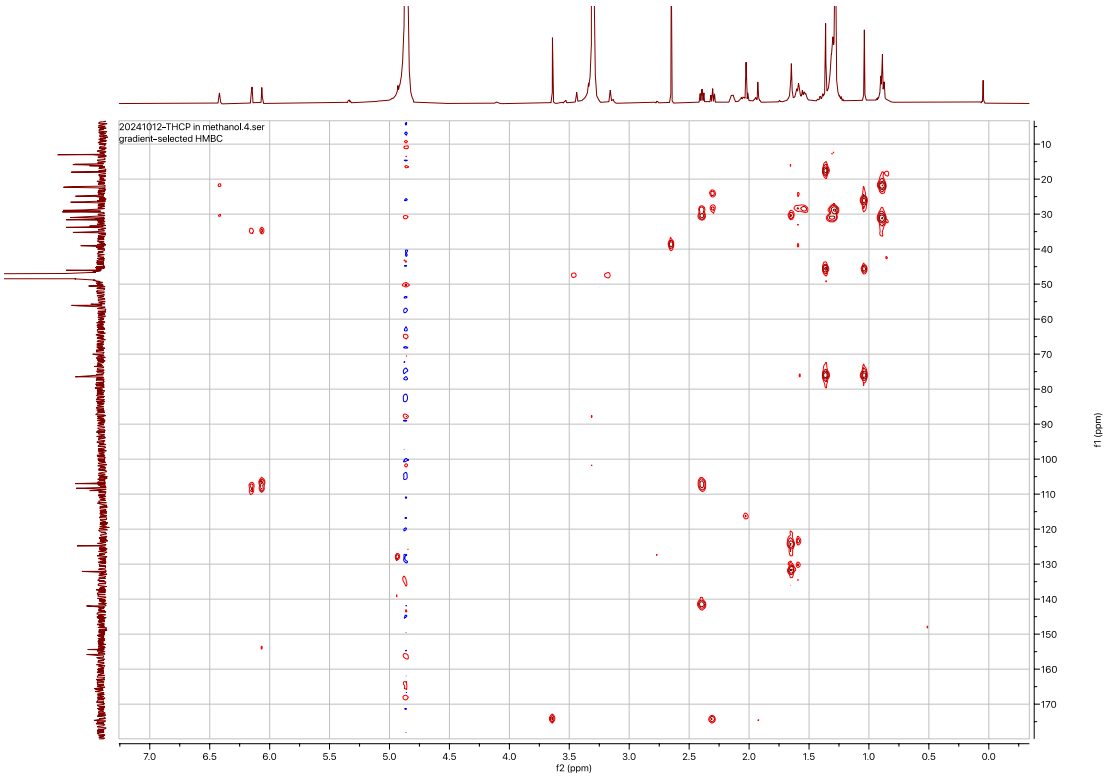

Figure S21 ^{1}H-^{13}C HMBC spectrum of compound Δ^{9} –THCP in CD_3OD (500 MHz)

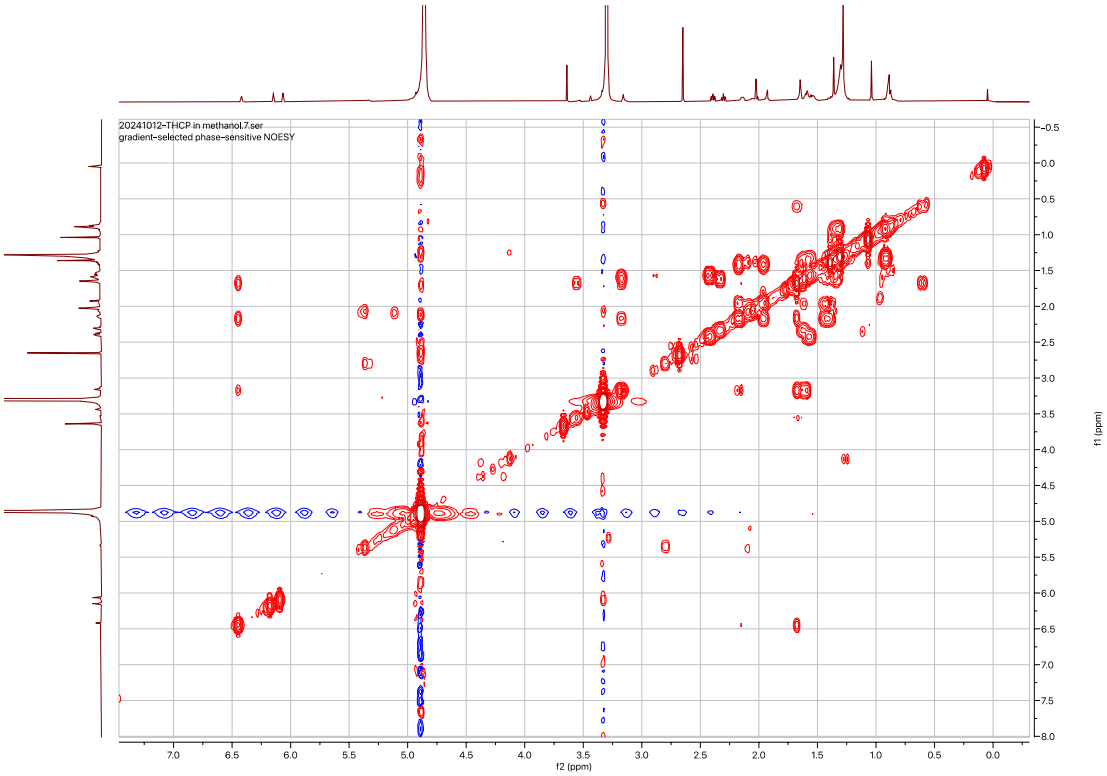

Figure S22 ^{1}H-^{1}H COSY spectrum of compound Δ^{9} –THCP in CD_3OD (500 MHz)

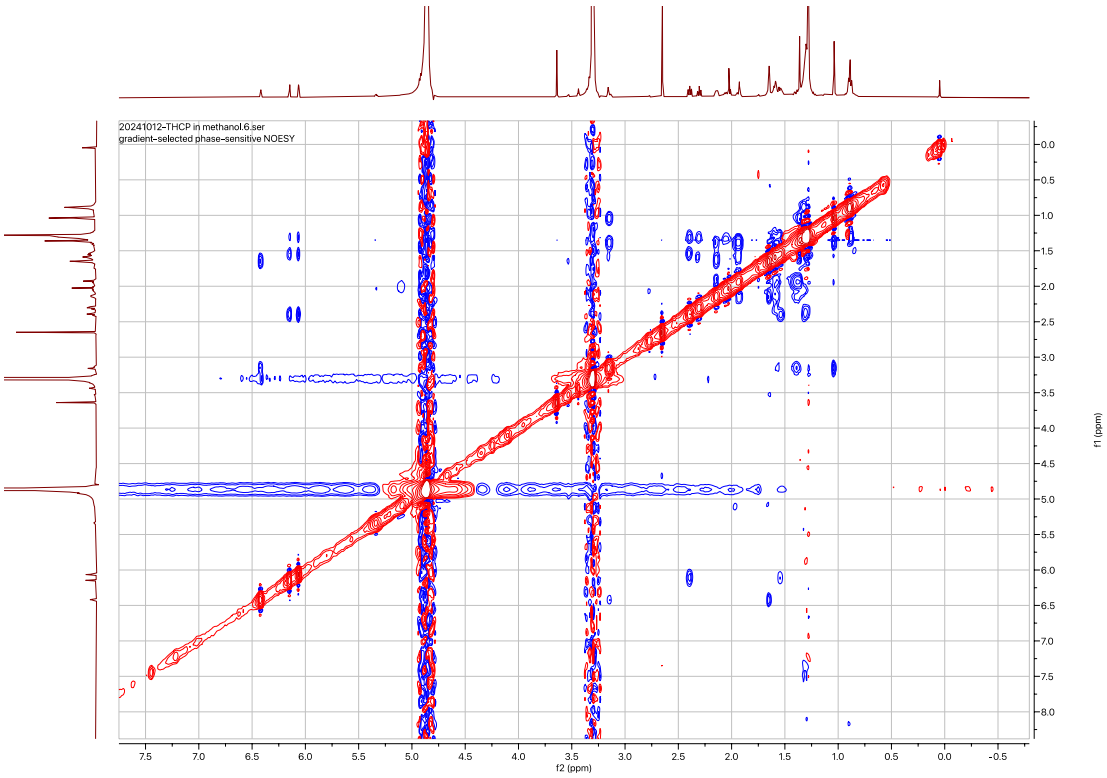

Figure S23 ^{1}H-^{1}H NOESY spectrum of compound Δ^{9} –THCP in CD_3OD (500 MHz)

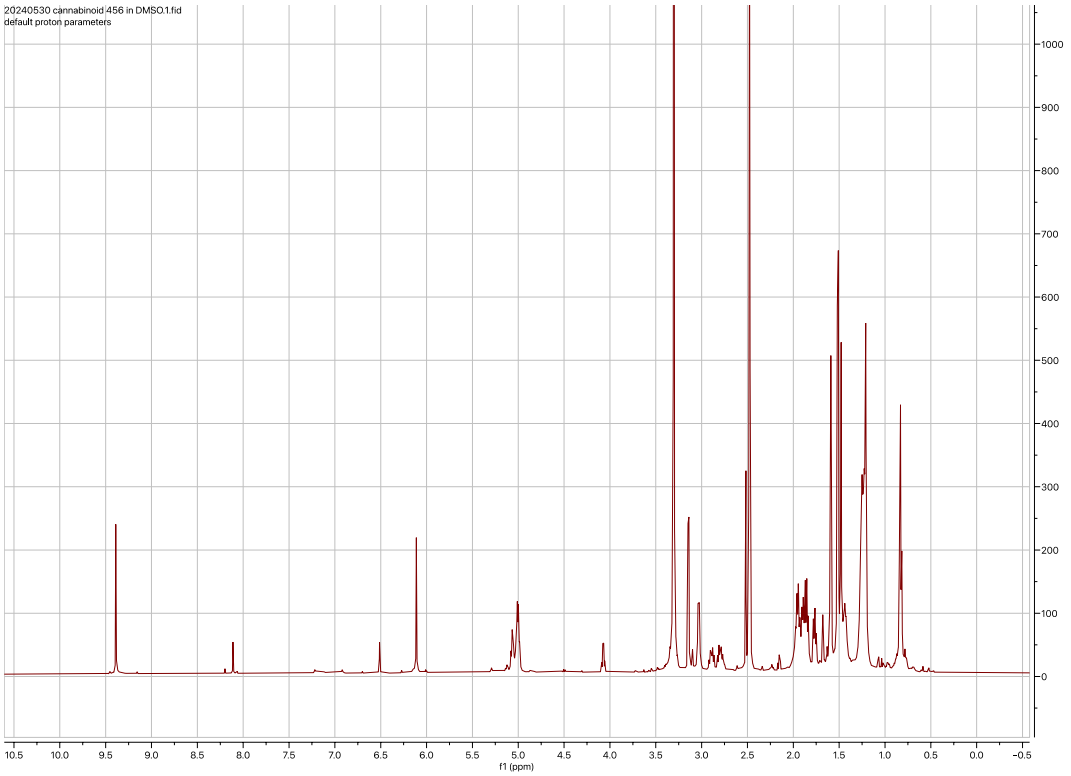

Figure S24 ^{1}H NMR spectrum of compound **3** in DMSO-*d*$_6$ (500 MHz)

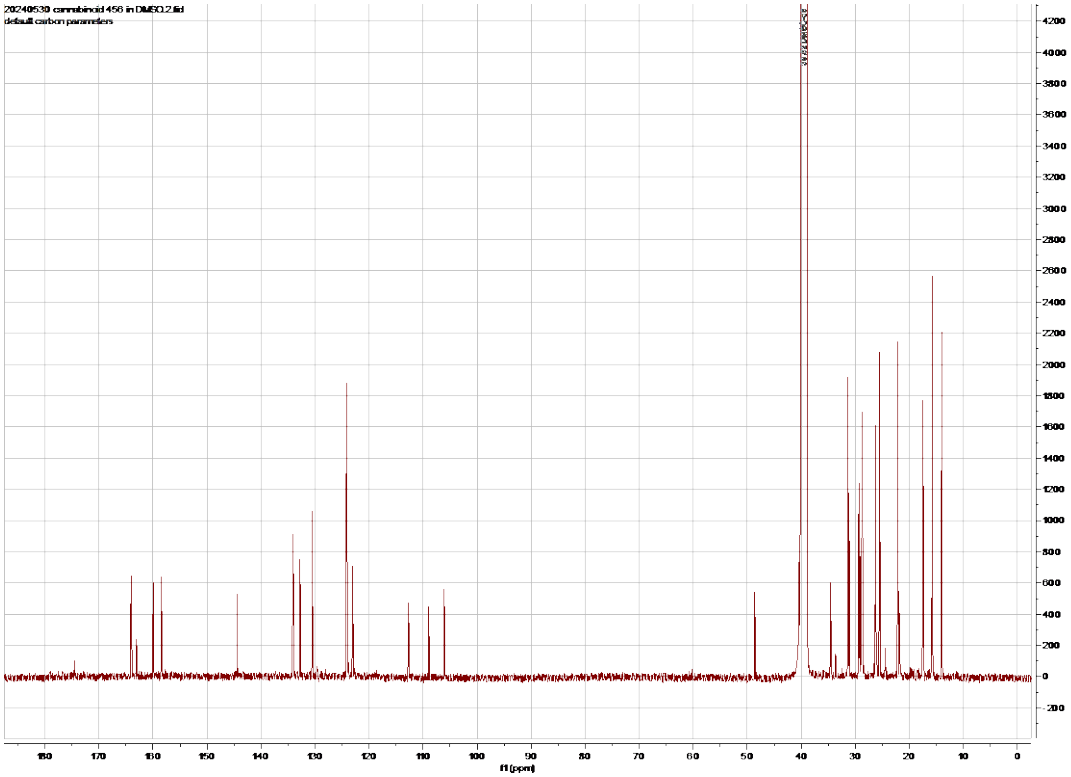

Figure S25 ^{13}C NMR spectrum of compound **3** in DMSO-*d*$_6$ (125 MHz)

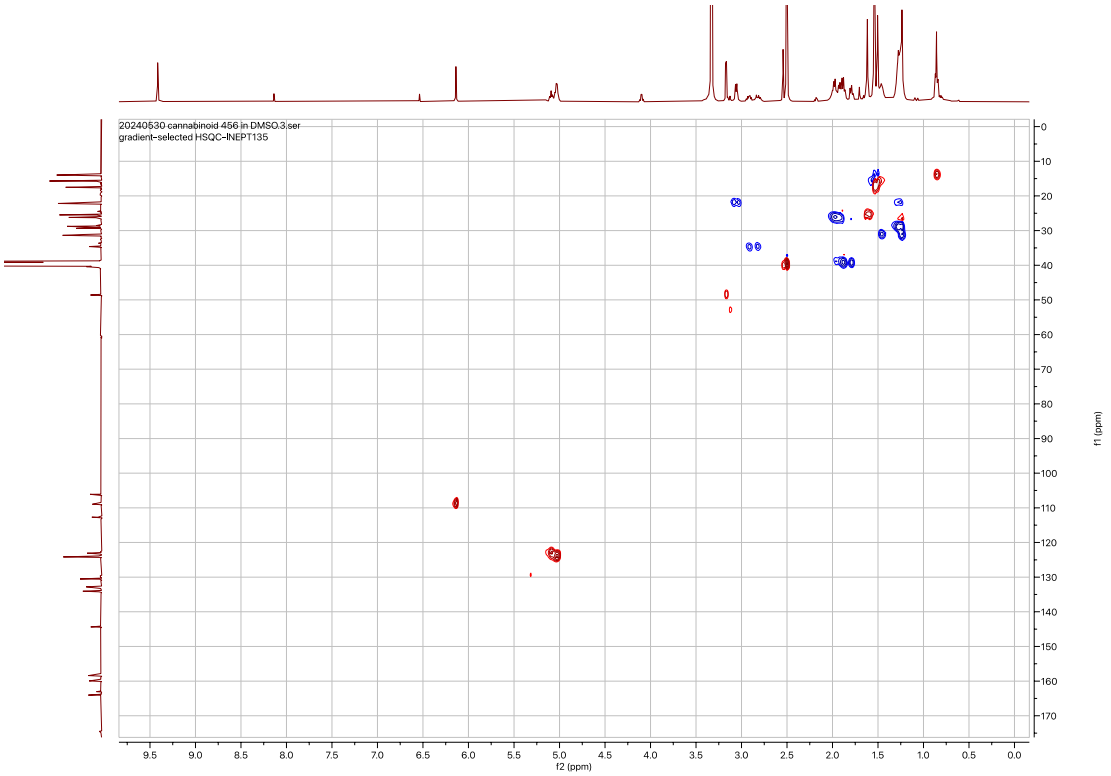

Figure S26 ^{1}H-^{13}C HSQC spectrum of compound **3** in DMSO-*d*$_6$ (500 MHz)

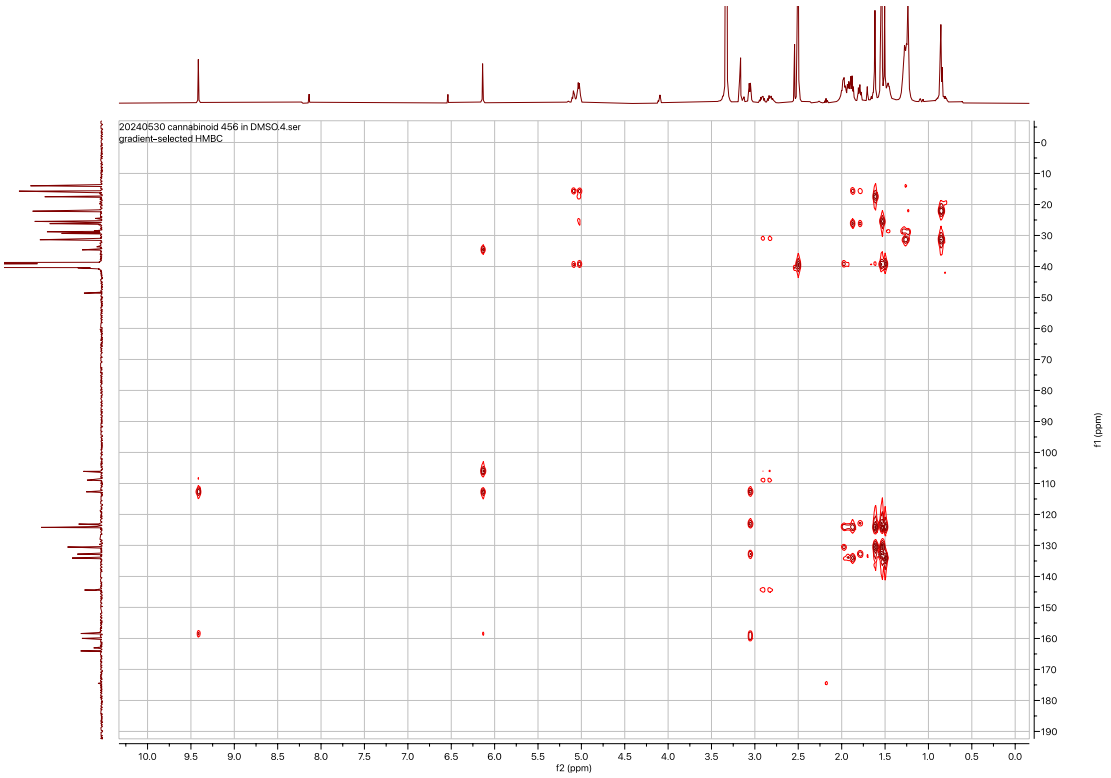

Figure S27 ^{1}H-^{13}C HMBC spectrum of compound **3** in DMSO-*d*$_6$ (500 MHz)

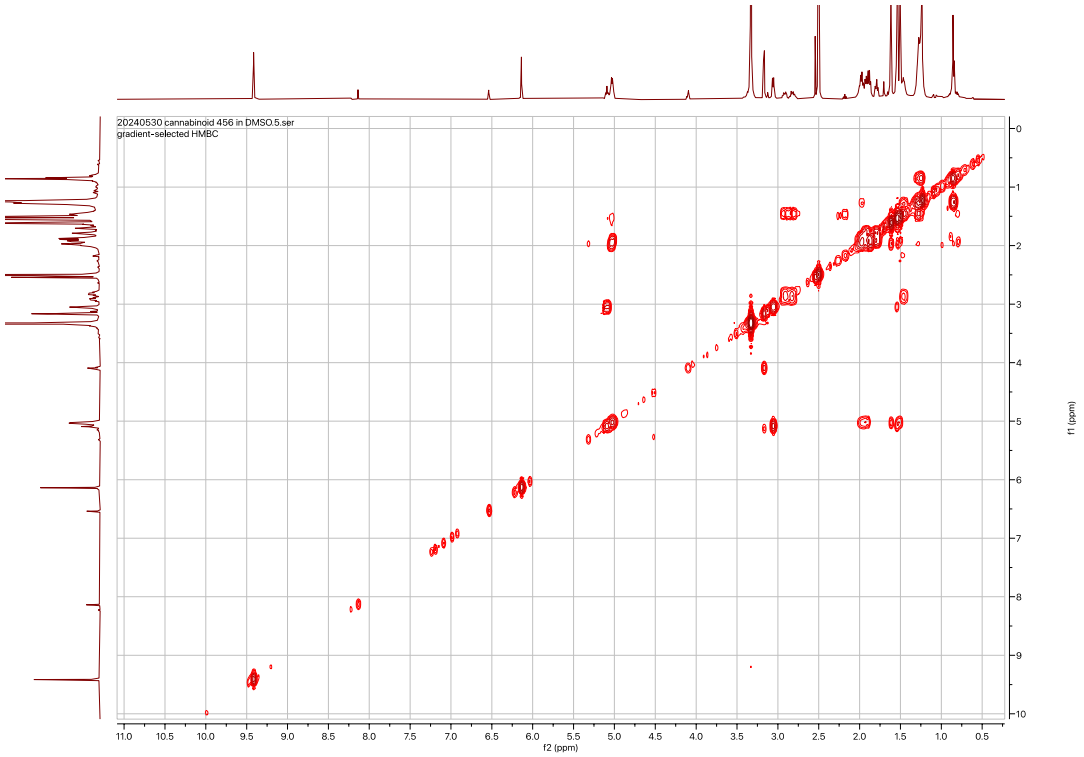

Figure S28 ^{1}H-^{1}H COSY spectrum of compound **3** in DMSO-*d*$_6$ (500 MHz)

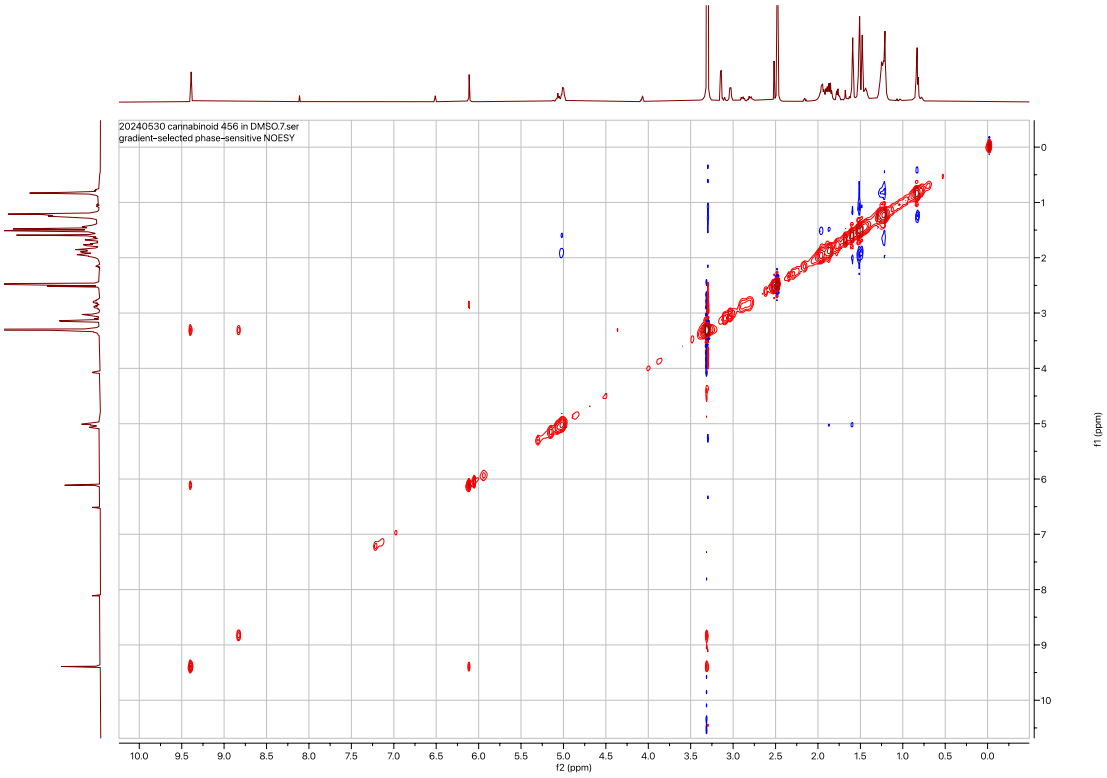

Figure S29 1H-1H NOESY spectrum of compound **3** in DMSO- *d*$_6$ (500 MHz)

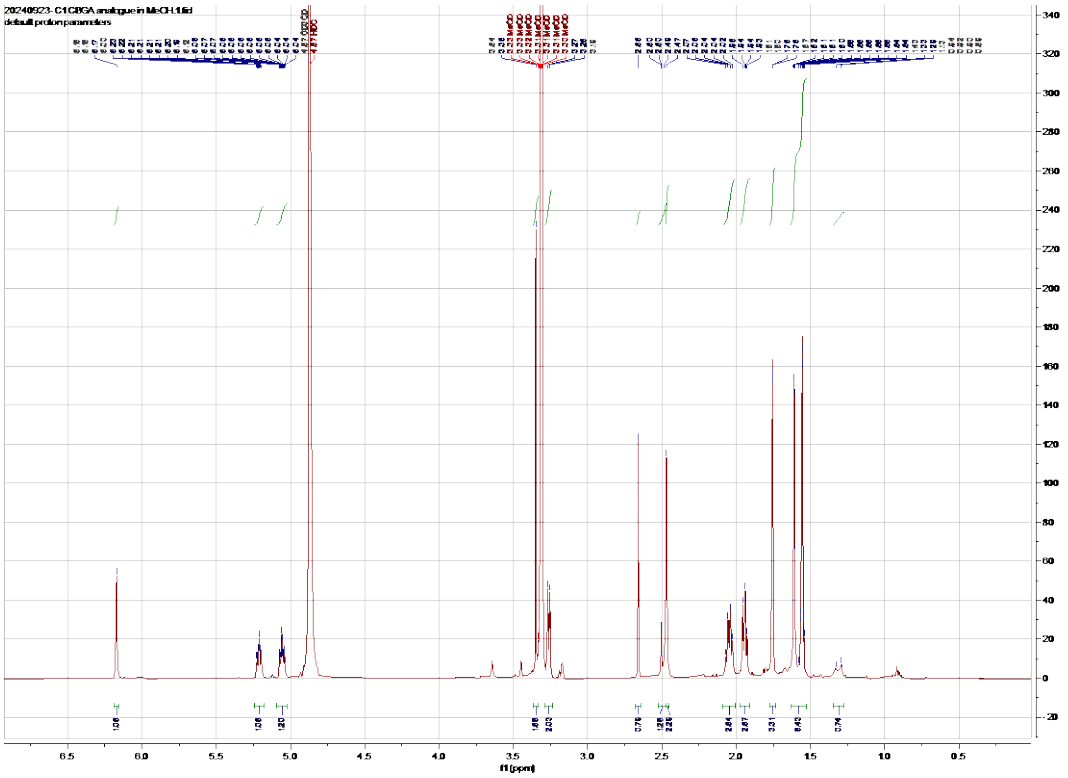

Figure S30 ^{1}H NMR spectrum of compound CBGCA in CD_3OD (500 MHz)

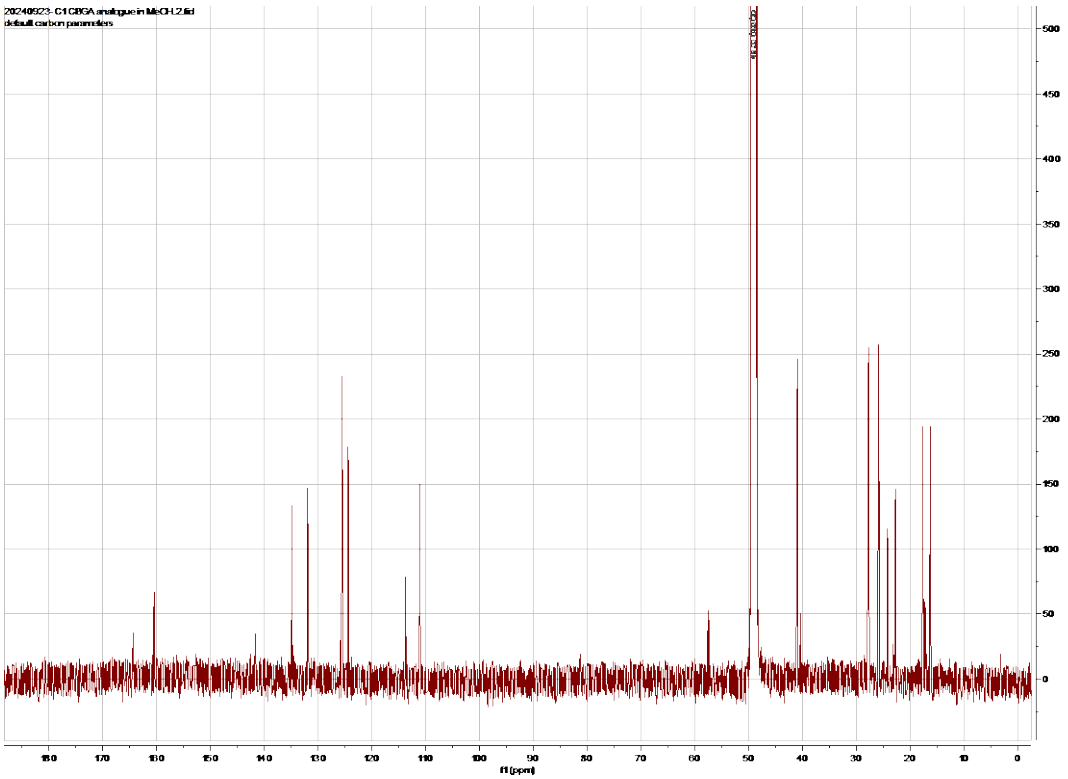

Figure S31 ^{13}C NMR spectrum of compound CBGCA in CD_3OD (125 MHz)

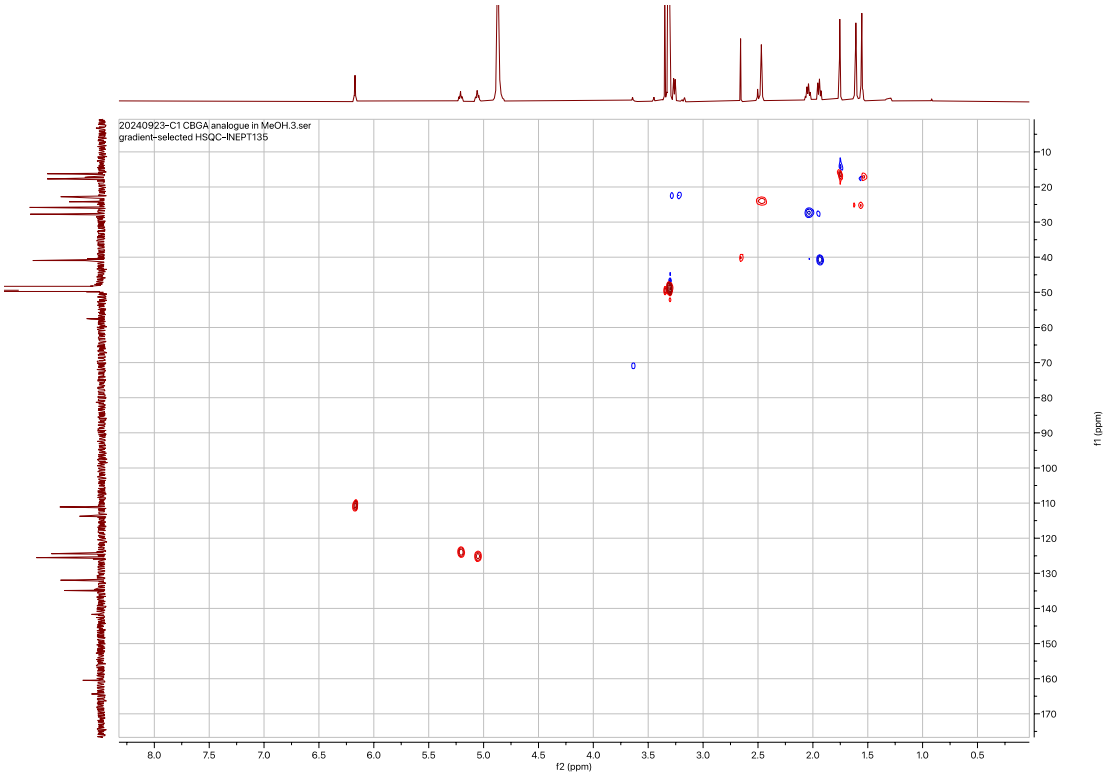

Figure S32 ^{1}H-^{13}C HSQC spectrum of compound CBGCA in CD_3OD (500 MHz)

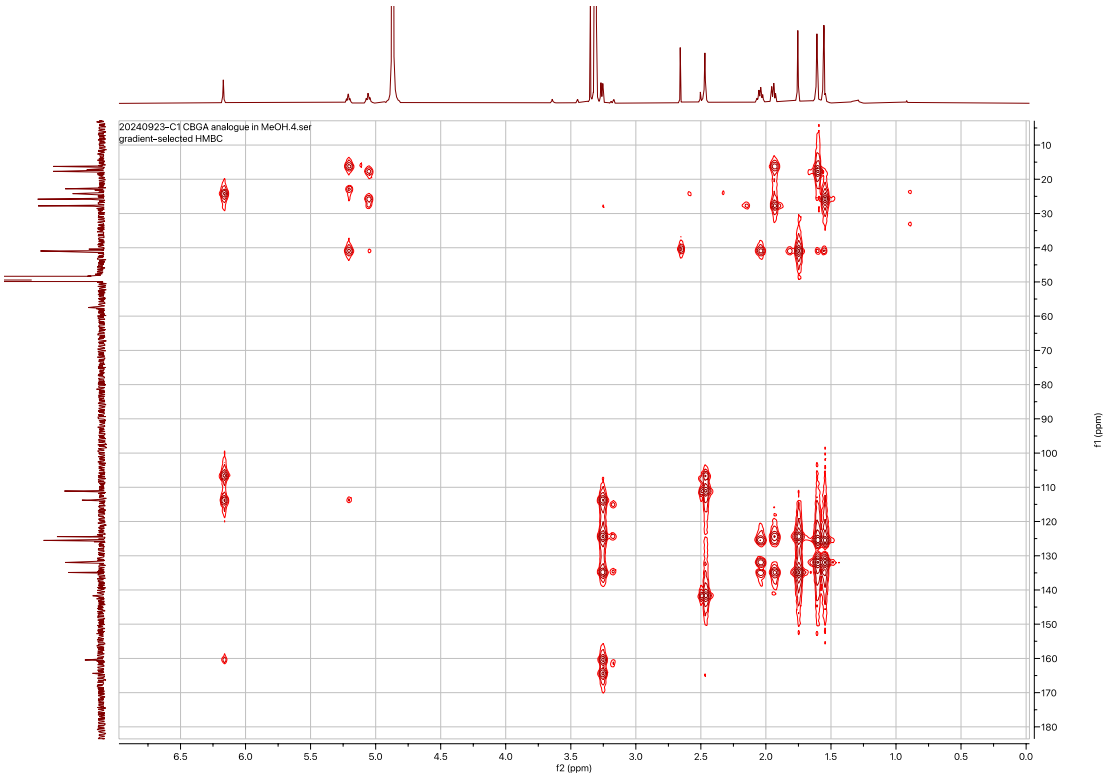

Figure S33 ^{1}H-^{13}C HMBC spectrum of compound CBGCA in CD_3OD (500 MHz)

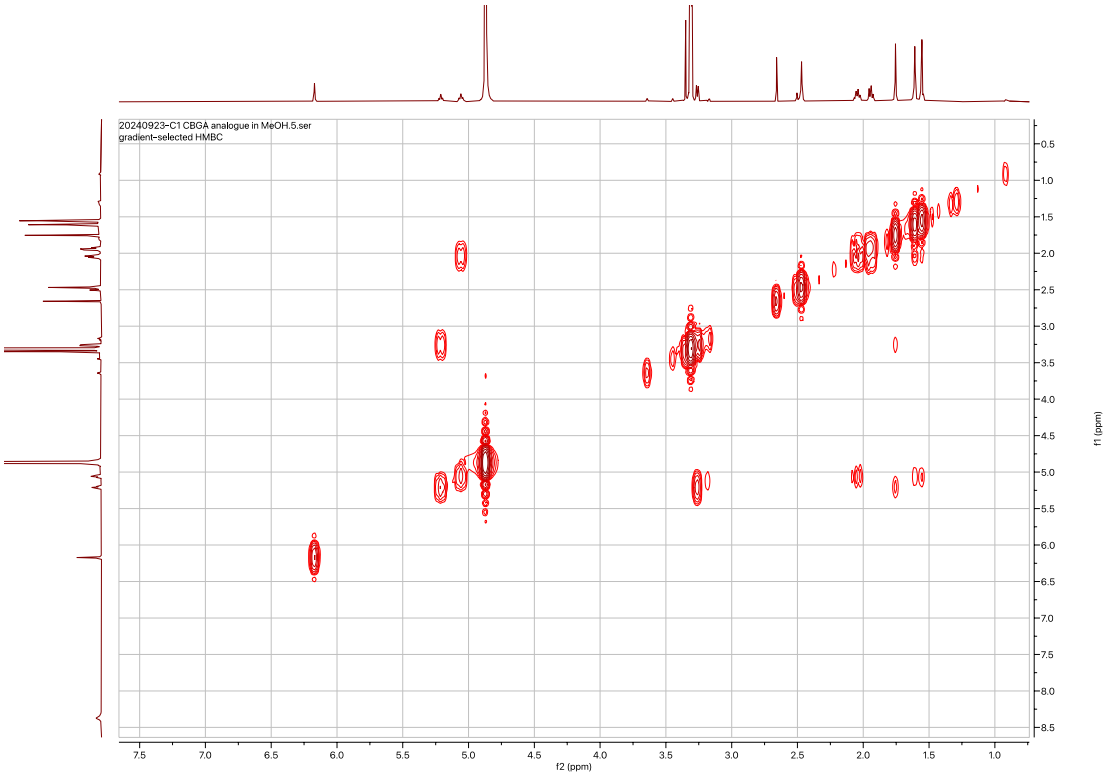

Figure S34 ^{1}H-^{1}H COSY spectrum of compound CBGCA in CD_3OD (500 MHz)

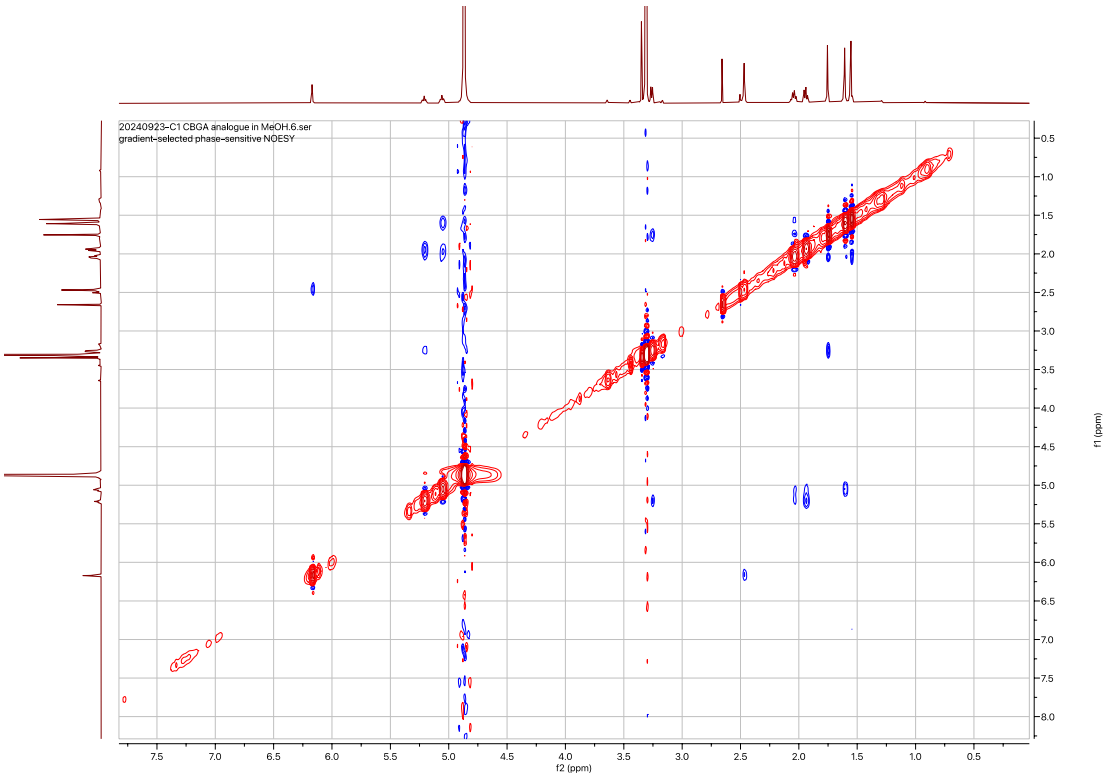

Figure S35 ^{1}H-^{1}H NOESY spectrum of compound CBGCA in CD_3OD (500 MHz)

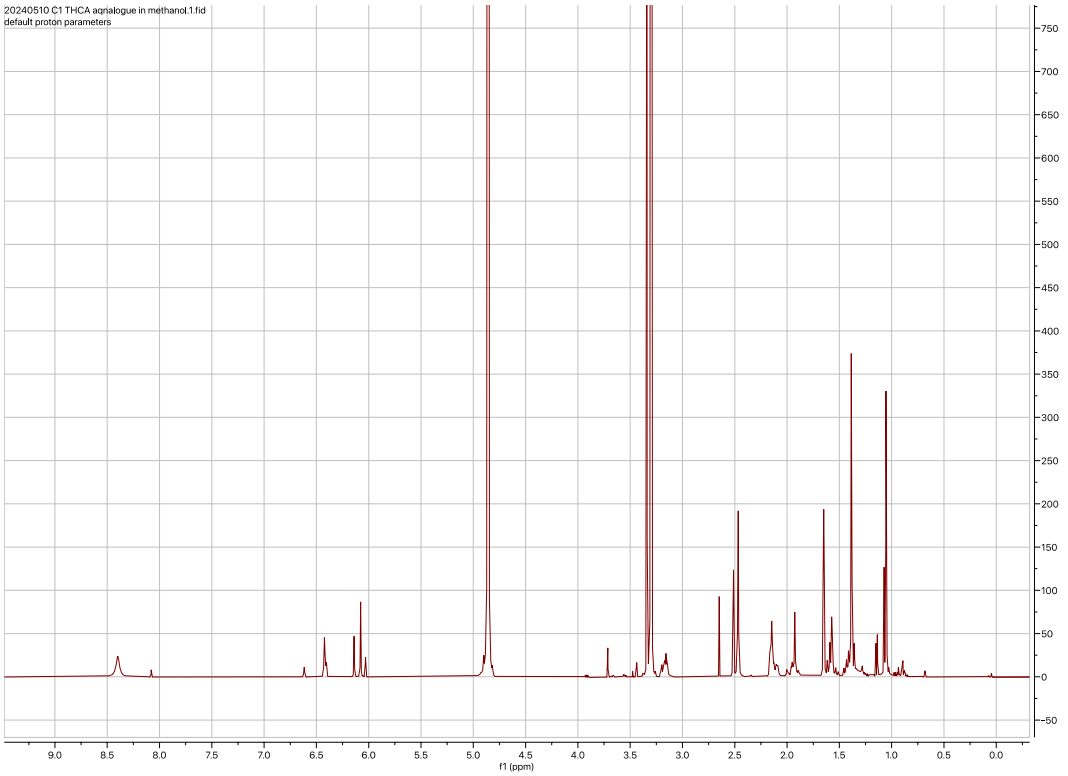

Figure S36 ^{1}H NMR spectrum of compound Δ^{9}–THCCA in CD_3OD (500 MHz)

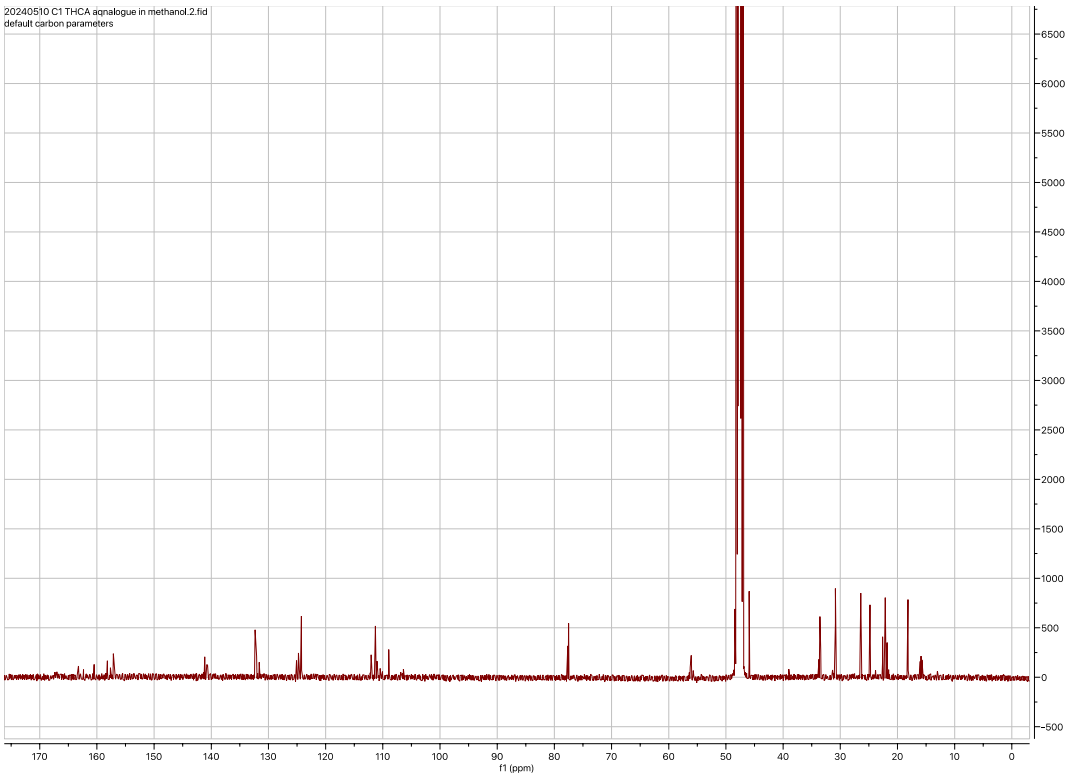

Figure S37 ^{13}C NMR spectrum of compound Δ^{9}–THCCA in CD_3OD (125 MHz)

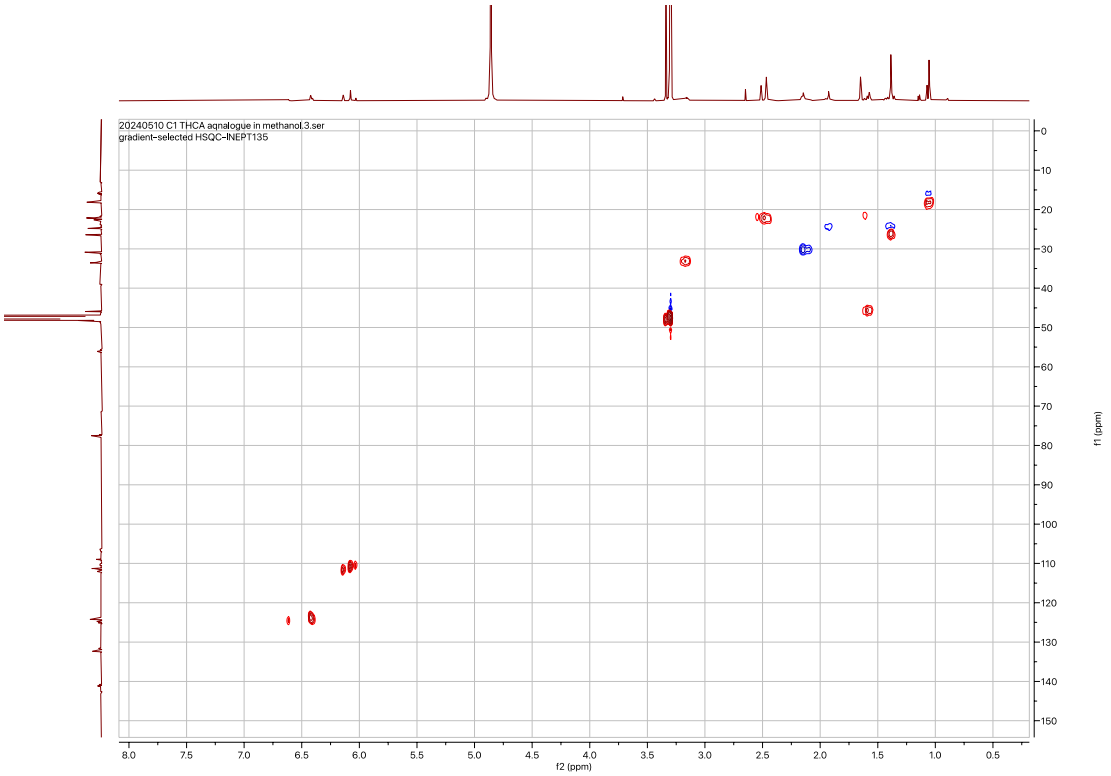

Figure S38 ^{1}H-^{13}C HSQC spectrum of compound Δ^{9}–THCCA in CD_3OD (500 MHz)

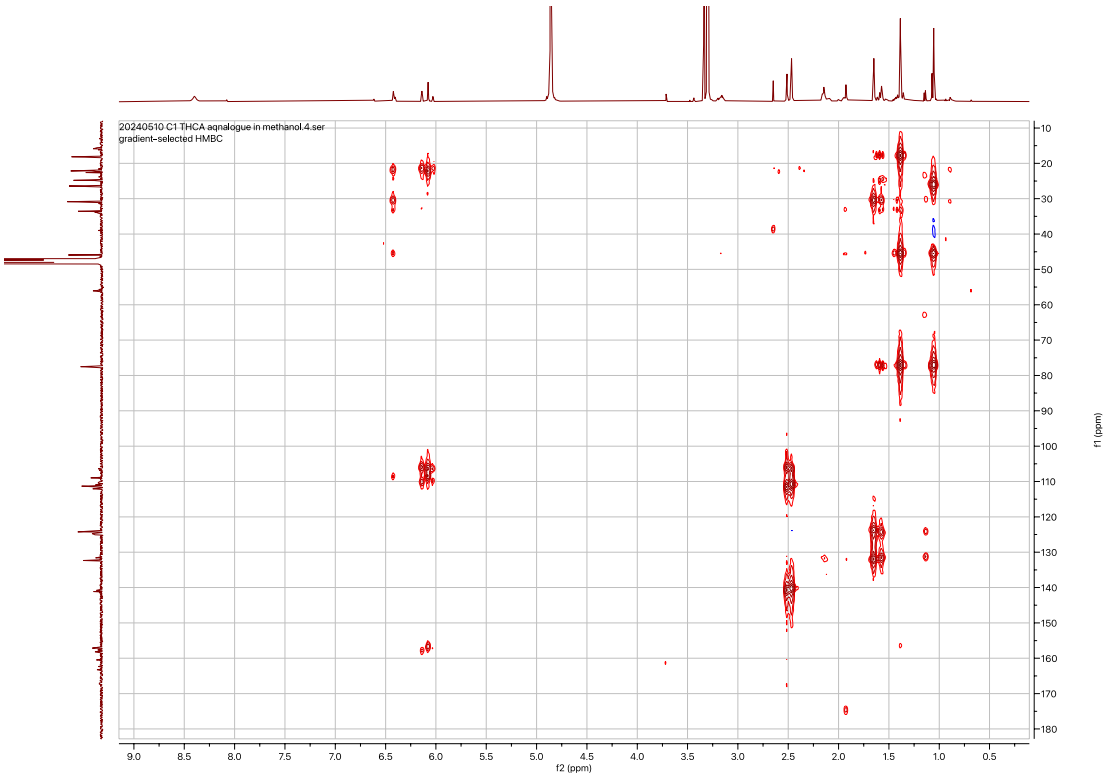

Figure S39 ^{1}H-^{13}C HMBC spectrum of compound Δ^{9}–THCCA in CD_3OD (500 MHz)

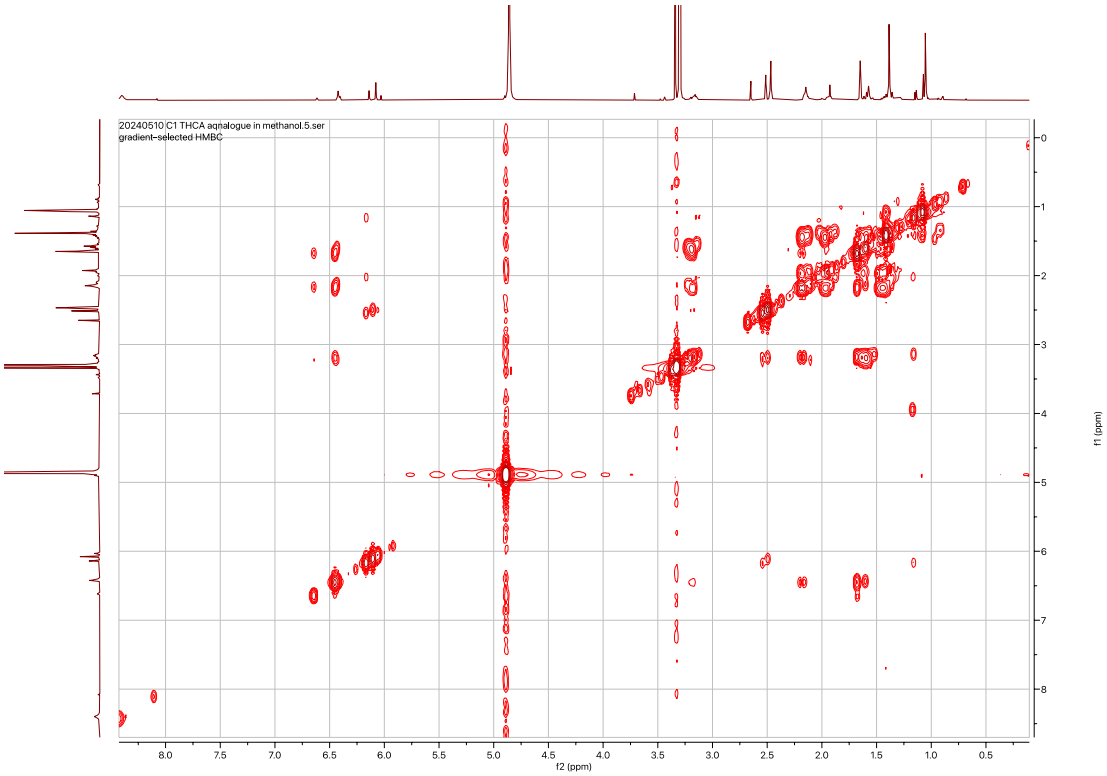

Figure S40 ^{1}H-^{1}H COSY spectrum of compound Δ^{9}–THCCA in CD_3OD (500 MHz)

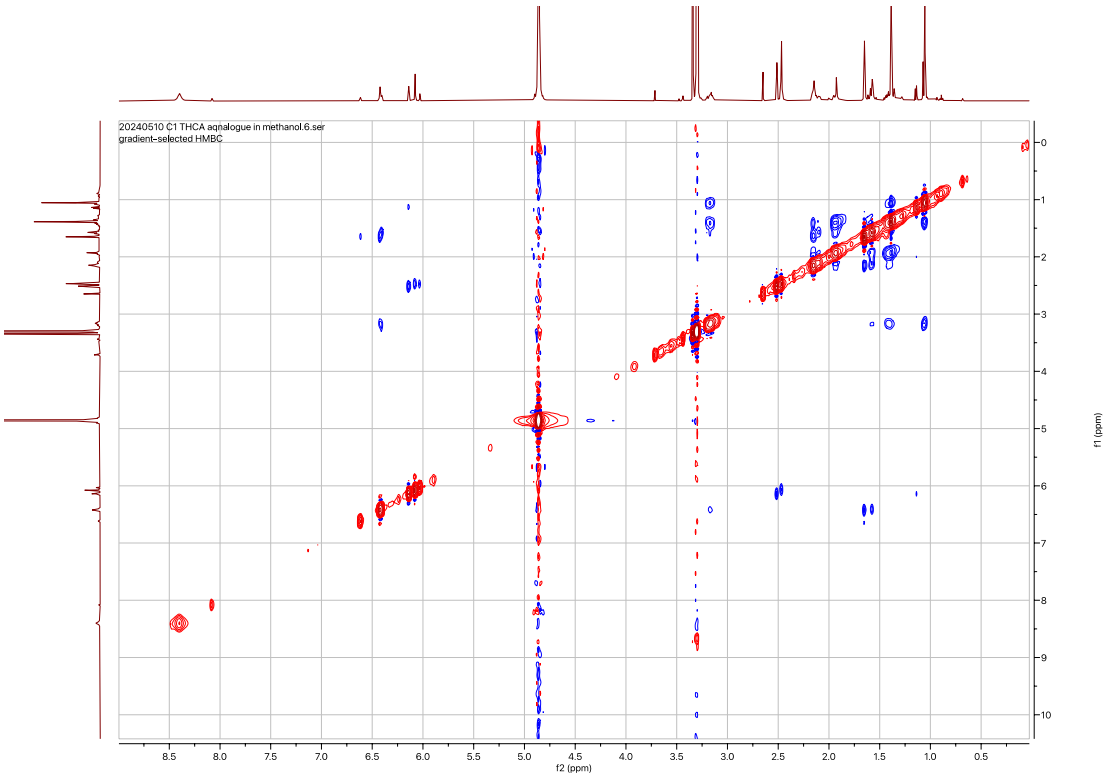

Figure S41 ^{1}H-^{1}H NOESY spectrum of compound Δ^{9}–THCCA in CD_3OD (500 MHz)

References

1. Yee, D. A.; Tang, Y. Investigating Fungal Biosynthetic Pathways Using Heterologous Gene Expression: Aspergillus Nidulans as a Heterologous Host. In *Methods in Molecular Biology*; Springer US: New York, NY, 2022; pp 41–52.
2. Harvey, C. J. B.; Tang, M.; Schlecht, U.; Horecka, J.; Fischer, C. R.; Lin, H.-C.; Li, J.; Naughton, B.; Cherry, J.; Miranda, M.; Li, Y. F.; Chu, A. M.; Hennessy, J. R.; Vandova, G. A.; Inglis, D.; Aiyar, R. S.; Steinmetz, L. M.; Davis, R. W.; Medema, M. H.; Sattely, E.; Khosla, C.; St. Onge, R. P.; Tang, Y.; Hillenmeyer, M. E. HEx: A Heterologous Expression Platform for the Discovery of Fungal Natural Products. *Sci. Adv.* **2018**, *4* (4).
3. Yee, D. A.; DeNicola, A. B.; Billingsley, J. M.; Creso, J. G.; Subrahmanyam, V.; Tang, Y. Engineered Mitochondrial Production of Monoterpenes in Saccharomyces Cerevisiae. *Metab. Eng.* **2019**, *55*, 76–84.
4. Jones, S.; Vignais, M.-L.; Broach, J. R. The *CDC25* Protein of *Saccharomyces Cerevisiae* Promotes Exchange of Guanine Nucleotides Bound to Ras. *Mol. Cell. Biol.* **1991**, *11* (5), 2641–2646.
5. Tang, S.; Wu, M. K. Y.; Zhang, R.; Hunter, N. Pervasive and Essential Roles of the Top3-Rmi1 Decatenase Orchestrate Recombination and Facilitate Chromosome Segregation in Meiosis. *Mol. Cell* **2015**, *57* (4), 607–621.
6. Cheng, W.; Li, W. Structural Insights into Ubiquinone Biosynthesis in Membranes. *Science* **2014**, *343* (6173), 878–881.
7. Yu, J.; Zhou, Y.; Tanaka, I.; Yao, M. Roll: A New Algorithm for the Detection of Protein Pockets and Cavities with a Rolling Probe Sphere. *Bioinformatics* **2010**, *26* (1), 46–52.